The Astrophysical Journal, 780:119 (20pp), 2014 January 10 doi:10.1088/0004-637X/780/2/119

TRANSFORMATION OF A VIRGO CLUSTER DWARF IRREGULAR GALAXY BY RAM PRESSURE STRIPPING: IC3418 AND ITS FIREBALLS

Jeffrey D. P. Kenney[1], Marla Geha[1], Pavel Jáchym[1,2], Hugh H. Crowl[3], William Dague[1], Aeree Chung[4], Jacqueline van Gorkom[5], and Bernd Vollmer[6]
[1] Yale University Astronomy Department, P.O. Box 208101, New Haven, CT 06520-8101, USA; jeff.kenney@yale.edu
[2] Astronomical Institute, Academy of Science of the Czech Republic, Bocni II 1401, 141 00 Prague, Czech Republic
[3] Bennington College, Bennington, VT, USA
[4] Department of Astronomy and Yonsei University Observatory, Yonsei University, 120-749 Seoul, Korea
[5] Department of Astronomy, Columbia University, 550 West 120th Street, New York, NY 10027, USA
[6] CDS, Observatoire astronomique de Strasbourg, UMR7550, 11 rue de l'université, F-67000 Strasbourg, France
Received 2013 August 1; accepted 2013 November 18; published 2013 December 16

ABSTRACT

We present optical imaging and spectroscopy and H I imaging of the Virgo Cluster galaxy IC 3418, which is likely a "smoking gun" example of the transformation of a dwarf irregular into a dwarf elliptical galaxy by ram pressure stripping. IC 3418 has a spectacular 17 kpc length UV-bright tail comprised of knots, head–tail, and linear stellar features. The only Hα emission arises from a few H II regions in the tail, the brightest of which are at the heads of head–tail UV sources whose tails point toward the galaxy ("fireballs"). Several of the elongated tail sources have Hα peaks outwardly offset by ~80–150 pc from the UV peaks, suggesting that gas clumps continue to accelerate through ram pressure, leaving behind streams of newly formed stars which have decoupled from the gas. Absorption line strengths, measured from Keck DEIMOS spectra, together with UV colors, show star formation stopped 300 ± 100 Myr ago in the main body, and a strong starburst occurred prior to quenching. While neither Hα nor H I emission are detected in the main body of the galaxy, we have detected 4×10^7 $M_\odot$ of H I from the tail with the Very Large Array. The velocities of tail H II regions, measured from Keck LRIS spectra, extend only a small fraction of the way to the cluster velocity, suggesting that star formation does not happen in more distant parts of the tail. Stars in the outer tail have velocities exceeding the escape speed, but some in the inner tail should fall back into the galaxy, forming halo streams.

Key words: galaxies: clusters: individual (Virgo) – galaxies: evolution – galaxies: interactions – galaxies: ISM

Online-only material: color figures

1. INTRODUCTION

Dwarf elliptical (dE)[7] galaxies are the dominant galaxy type (by number) in clusters (Binggeli et al. 1987), although their origin has not been well understood (Ferguson & Binggeli 1994; Conselice et al. 2001; Geha et al. 2003). Since gas-poor dEs are preferentially found in cluster centers, whereas gas-rich dwarf irregulars (dIs) are usually found in cluster outskirts and outside of clusters (Binggeli et al. 1987), a natural origin for dEs is via gas stripping of dIs as they fall into dense intracluster medium (ICM) gas near the center of a cluster. Many papers over the years have discussed the significant evidence supporting some version of this scenario (Lin & Faber 1983; Lee et al. 2003; van Zee et al. 2004a, 2004b; Lisker et al. 2006a, 2006b; Boselli et al. 2008; De Rijcke et al. 2010; Kormendy & Bender 2012) although properties of many dEs that cannot be explained by ram pressure alone (kinematics, shape, nuclei, metallicity) has naturally led to questions on the role of ram pressure stripping in dwarf galaxy evolution (Ferguson & Binggeli 1994; Conselice et al. 2001). This clearly indicates that ram pressure stripping is not the only mechanism important for producing many of the current dEs and that gravitational interactions must play a role, but the complexity has made it hard to clearly confirm the role of ram pressure stripping.

What has been lacking are clear examples of galaxies undergoing such a dI→dE transformation. We propose that in the Virgo Cluster dwarf IC3418, we are witnessing a critical stage in the transformation of a dI into a dE, the recent and rapid removal of the entire interstellar medium (ISM) by ICM ram pressure stripping.

2. THE GALAXY IC3418

IC3418 (VCC1217) is a peculiar dI galaxy (IBm?; de Vaucouleurs et al. 1991) notable for an unusual UV-bright one-sided tail (Gil de Paz et al. 2007; Chung et al. 2009; Hester et al. 2010; Fumagalli et al. 2011), but highly deficient in H I (Hoffman et al. 1989; Chung et al. 2009) and CO emission (Jáchym et al. 2013). It is located close in projection ($1.^\circ0 \simeq 277$ kpc $\simeq 0.17R_{\rm vir}$; McLaughlin 1999) to M87 at the core of the Virgo Cluster.

IC3418 has a line-of-sight velocity of 176 ± 15 km s^{-1} (Section 4.1.2), consistent with a distance anywhere from the Local Group to the Virgo Cluster. There is no current distance estimate for the galaxy; however, the smoothness of the starlight in the main stellar body indicates that IC3418 is beyond the Local Group, since the pixel-to-pixel variation in brightness is much less in IC3418 than in Local Group galaxies. It is mostly on this basis, which is essentially the surface brightness fluctuation method, that Binggeli et al. (1985) considered IC3418 a true member of the Virgo Cluster. In this paper, we adopt a distance

[7] In this paper we will follow the majority of recent authors and refer to the more massive early type dwarf galaxies as dEs, and lower mass ones as dwarf spheroidals (dSphs). However, some authors (Kormendy & Bender 2012) prefer the name spheroidal (Sph) for more massive early type dwarfs, since they are distinct systems from giant ellipticals, and dEs (or Sphs) and dSphs seem to be part of the same family. dE can be interpreted as "early type dwarf."

of 16.7 Mpc, equal to the mean distance of galaxies in the M87 subcluster (cluster A) of Virgo (Mei et al. 2007). Given its blueshift of 900 km s^{-1} with respect to the mean Virgo velocity of 1079 km s^{-1} (NASA/IPAC Extragalactic Database) IC3418 is moving at high speed through the Virgo Cluster toward us. Its tail should therefore be behind the main body of the galaxy and should be located further from us.

With a blue magnitude of $B_T \simeq 14.5$ and $M_B \simeq -16.5$, H-band luminosity $= 8.7 \times 10^8\ L_\odot$ (from GOLDMINE; Gavazzi et al. 2003), and a stellar mass of $4 \times 10^8\ M_\odot$ (Fumagalli et al. 2011), it is among the brighter and more massive dwarfs in the cluster. Its optical luminosity and stellar mass are about twice that of the Small Magellanic Cloud, and an order of magnitude less than NGC 4522, a Virgo Cluster spiral galaxy with clear evidence for ongoing ram pressure stripping (Kenney et al. 2004).

The optical and NUV–H colors (from GOLDMINE; Gavazzi et al. 2003) of the main body of the galaxy place it within the blue cloud of galaxies (Hester et al. 2010; Fumagalli et al. 2011) although its NUV–FUV colors are intermediate between the major "blue" and "red" galaxy populations (Hester et al. 2010; Fumagalli et al. 2011), implying significant star formation until the last few hundred Myr.

In recent papers, Hester et al. (2010) and Fumagalli et al. (2011) discussed UV and optical imaging of IC3418, in which they presented evidence that the galaxy is ram pressure stripped, that the remarkable tail originates from star formation within ram pressure stripped gas, and that the galaxy is evolving from the blue cloud to the red sequence. In this paper, we confirm and extend their main conclusions. We present the first kinematic study of the tail features and provide important new information on the morphologies and stellar populations of the tail features and the main body. We emphasize that IC3418 is a clear example of a dwarf galaxy being transformed from a dI into a dE by ram pressure stripping, and we make the case that ram pressure stripping is the decisive process in converting dIs into dEs.

3. OBSERVATIONS AND DATA REDUCTION

3.1. WIYN *BVR* Hα Imaging

Exposures of IC 3418 were taken in *BVR* and narrowband Hα+[N II] filters on the 3.5 m WIYN telescope[8] at KPNO in 2009 March. We used the 4096 × 4096 pixel Mini-Mosaic imager, which has two CCDs, and a plate scale of 0.″14 pixel^{-1}, giving a field of view of 9.′6 (42 kpc). For the Hα imaging, we used a narrowband filter (W36) with a bandwidth of 60 Å centered on 6576 Å. This filter includes the redshifted Hα and the two straddling [N II] lines.

Integration times totalled 24 minutes for *V* and *R*, 35 minutes for *B*, 56 minutes for the Hα+[N II] narrowband filter, and they were divided up into five or more dithered exposures per filter. The seeing for all images used ranged between 0.″8 and 1.″0.

We used the "mscred" package within IRAF to bias-subtract, flat-field, register, and combine the images for each filter. Flat fielding was done using both domeflats and skyflats produced from object images taken throughout the night. Cosmic rays were removed using the pixel rejection routines in the combine task. After sky subtraction, the *R*-band image was scaled and then subtracted from the narrowband filter image to obtain a continuum-free Hα+[N II] (hereafter referred to as Hα) image.

3.2. Keck Optical Spectroscopy: LRIS

Optical spectroscopy of IC 3418 to study its stellar population was obtained with the LRIS spectrograph on the Keck I telescope on 2009 February 26–27. The data presented here use the blue 600/4000 grism to achieve wavelength coverage of 3400–5500 Å and spectral resolution of 6.1 Å FWHM. Our observations utilize a custom slitmask 1.″5 wide and 5.′6 long, with 2″ supports placed every 54″. The seeing at the start of the night was 0.″8. The slit was placed such that it covered the entire optical extent of the galaxy and, on one side, extended well beyond the galaxy to measure the sky emission. The slit was oriented at 50°, close to the major axis of the galaxy. Six exposures each of length 1200 s were taken, for a total exposure time of 7200 s.

The data were bias-corrected and flat-fielded using standard data reductions techniques and IRAF packages. Following this, spatial distortions in the two-dimensional spectrum were removed using the IRAF package TRANSFORM. This correction ensures that spectra could be reliably extracted from the smooth light profile of the galaxy. These extracted one-dimensional spectra were then wavelength corrected using mercury–cadmium–zenon arc lamps and had their sky signal subtracted using data from the end of the slit, well beyond the optical extent of the galaxy.

3.3. Keck Optical Spectroscopy: DEIMOS

Optical spectroscopy of IC 3418 and its tail to study their kinematics was obtained with the DEIMOS spectrograph (Faber et al. 2003) on the Keck II 10 m telescope on 2010 February 14. One mask was observed with the 1200 line mm^{-1} grating covering a wavelength region 6400–9100 Å. The spectral dispersion of this setup was 0.33 Å pixel^{-1}, equivalent to $R =$ 6000 for our 0.″7 wide slitlets, or a FWHM of 1.37 Å. The spatial scale was 0.″12 per pixel. Three exposures were taken, with a total exposure time of 3000 s.

Spectra were reduced using a modified version of the `spec2d` software pipeline (version 1.1.4) developed by the DEEP2 team at the University of California-Berkeley for that survey. A detailed description of the reductions can be found in Geha et al. (2010). The final one-dimensional spectra were rebinned into logarithmic wavelength bins with 15 km s^{-1} per pixel. Radial velocities were measured by cross-correlating the observed science spectra with a series of high signal-to-noise stellar templates. We applied a heliocentric correction to all velocities presented in this paper.

Our observations utilize a custom slitmask with a series of slits oriented at position angle (P.A.) = 135°, corresponding to the tail axis and approximately the minor axis of the galaxy. One slit of 1.′6 length passed near the center of the galaxy and includes the object S5 which is projected near the galaxy center. Other shorter slits were centered on the brightest features in the tail, including most of those with Hα emission detected in the imaging, plus some UV sources with little or no Hα emission (U1, U3, U4). In addition, we covered a couple of stars and background galaxies in the field.

The velocity of this galaxy has been uncertain. We measure the heliocentric velocity unambiguously from the absorption lines in the Keck DEIMOS spectra to be 176 ± 15 km s^{-1} (Section 4.1.2).

[8] The WIYN Observatory is a joint facility of the University of Wisconsin-Madison, Indiana University, Yale University, and the National Optical Astronomy Observatories.

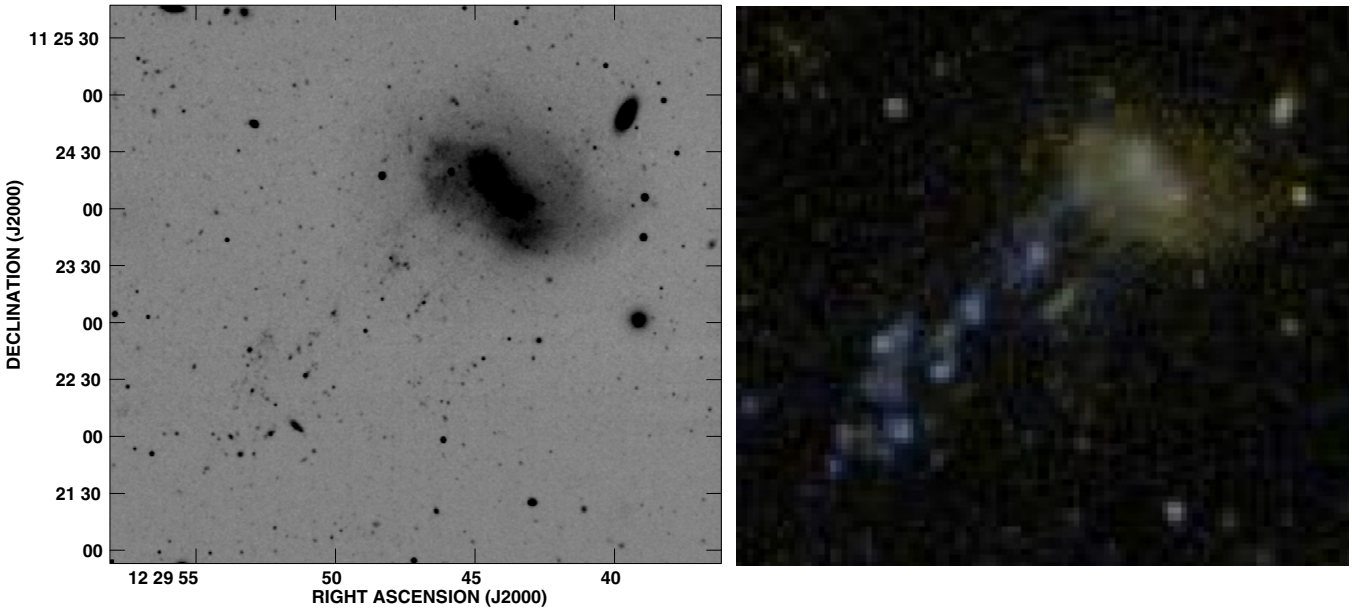

Figure 1. Comparison of IC3418 in optical and UV. Right: WIYN *B*-band image of IC 3418, showing irregular structure in main body of galaxy and numerous faint stellar associations in a tail extending to SW. Left: *GALEX* NUV+FUV color image of IC 3418, reproduced from Hester et al. (2010). FUV is blue, NUV is red, and the average UV intensity is green. The bright UV emission from the tail indicates recent and ongoing star formation from gas clouds which were presumably ram pressure stripped from the main body of the galaxy. Field of view in both images is $\sim 5' \times 5'$. The tail stands out from the background much more in the UV than the optical since the tail stars are young.

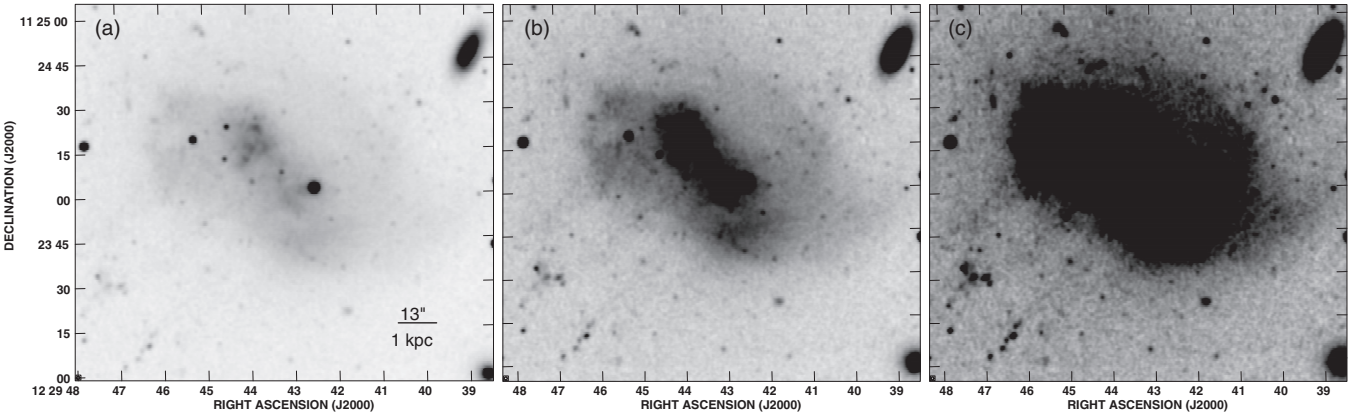

Figure 2. WIYN *B*-band images of IC 3418, with different stretches to highlight different regions of the main body of the galaxy. (a) Shallow image showing star formation substructure in central $r = 2$ kpc. (b) Medium image showing spiral arms and NW/SE brightness asymmetry over $r = 2$–4 kpc. (c) Deeper image showing spiral arm feature in outer disk plus the inner part of the tail.

4. RESULTS

4.1. Main Body of IC3418

4.1.1. Imaging Analysis of Main Body

A *B*-band image of the main body and tail of IC3418 is shown in Figure 1, and *B*-band images of the main body are shown at different stretches in Figure 2. Overall the images show a low surface brightness galaxy with substructure indicating recent star formation.

Figure 2(a) shows a bright complex of arcs and other features, ~1 kpc in extent, located ~1 kpc northeast (NE) of the galaxy center. A second, fainter complex of similar size, exists ~0.7 kpc southwest (SW) of the center (and E of the very bright star S6). The central $r \simeq 2$ kpc region is somewhat bluer in both the optical and the UV than the surrounding regions (Hester et al. 2010; Fumagalli et al. 2011), indicating more recent star formation here.

Figure 2(b) shows that at a surface brightness level which encompasses these two young stellar complexes, the galaxy shows an elongated lima-bean shaped distribution resembling an irregular bar with length ~2 kpc, which might be the origin of the bar classification by the RC3. There is no clear evidence for a stellar bar, and since the direction of elongation is perpendicular to the tail, the elongation could be a result of ram pressure. The disk from $r = 2$–5 kpc (Figure 2(b) and (c)) shows spiral structure, further evidence that IC3418 is a disk system. At these radii, the southeast (SE; tail) side of the main body is brighter and bluer than the northwest (NW) side, perhaps due to recently formed stars in ram pressure stripped gas contributing additional blue light at the base of the tail.

Despite substructure in optical images resembling star-forming regions, the Hα image shows no emission from the main body of the galaxy, down to a 3σ sensitivity limit of 2.1×10^{-17} erg s^{-1} cm^{-2} arcsec^{-2}, which is 2.3 times deeper than Fumagalli et al. (2011). This corresponds to a point source Hα

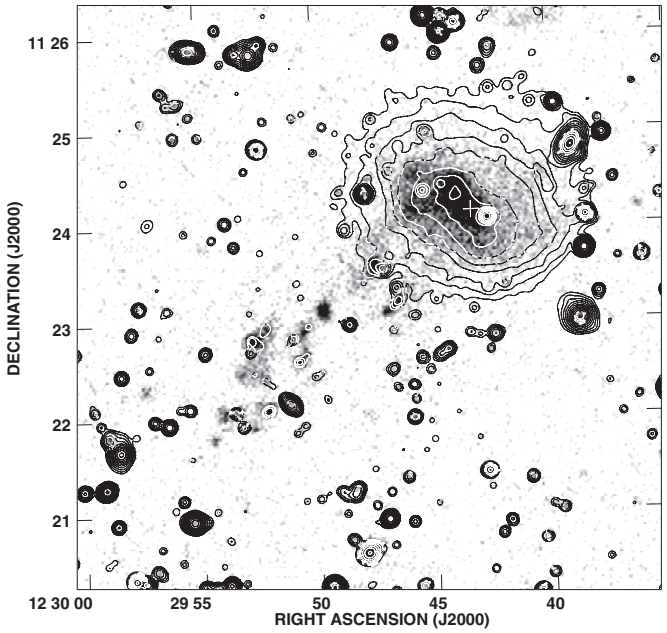

Figure 3. WIYN *R*-band image of IC 3418 convolved to 5″ resolution, superposed on NUV image. The deep *R*-band image shows a fairly regular stellar distribution at large radii and no smooth stellar component to the tail, indicating that a tidal interaction is not responsible for the tail. Outermost contour level is 26.5 mag arcsec^{-2}, and contour increment in 0.5 mag arcsec^{-2}. Location of Object S5, possibly a nuclear star cluster, is marked with a cross.

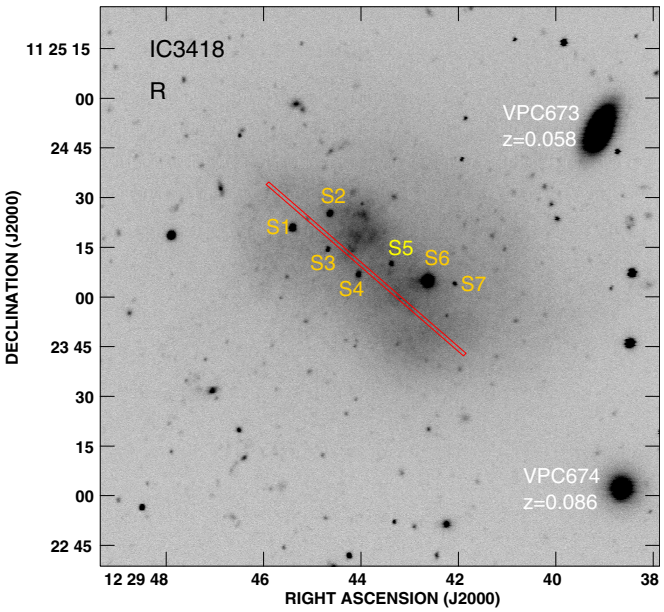

Figure 4. WIYN *R*-band image of main body of IC 3418, with bright stars and star-like objects toward or in IC3418 identified. Object S5 has the velocity of IC3418, so it is in the galaxy. It is located within a few arcseconds of the center and could be the nucleus. The other objects are either foreground stars, supergiants in IC3418, or globular clusters (see Section 4.1.2). The position of the central ±40″ of the Keck LRIS slit used for the stellar population analysis is marked.

(A color version of this figure is available in the online journal.)

luminosity of 7×10^{35} erg s^{-1}, which is an order of magnitude fainter than the Orion Nebula. H I emission (Hoffman et al. 1989; Chung et al. 2009) is also undetected in the main body of the galaxy. The only Hα and H I emission detected are in the tail, which we discuss in Sections 4.2.1 and 4.2.2. There is a marginal CO(2–1) detection suggesting a small amount ($\sim 10^6\ M_\odot$) of molecular gas but only from the central few arcseconds (Jáchym et al. 2013) and not from the young stellar complexes. There is a suggestion of dust extinction in panels (b) and (c) of Figure 2, on the SE side near the base of the tail, where there is less light than at other regions at the same radii, although these surface brightness variations might also be due to disk structure. There are only upper limits on dust emission from IC3418 (Jáchym et al. 2013).

In Figure 3 we show a "deep" optical image, our WIYN *R*-band image convolved to 5″ resolution. Residual flat-fielding errors may affect the outermost contour on the west side of the galaxy (right side of figure), but otherwise, the contour levels are robust. This smoothed image reaches a surface brightness of 26.5 mag arcsec^{-2}. At this level, shown by the outermost contours in Figure 3, the main body is seen to extend out to at least 80″ = 6.2 kpc, which is roughly twice the RC3 isophotal diameter. The isophotes in the outer galaxy suggest a disk with P.A. $\simeq 50^\circ$ and inclination $\simeq 30^\circ$. The outer isophotes are fairly regular, with no evidence for tidal features. The light from the main body encompasses $\sim 1/3$ the tail; however, there are no suggestions of a smooth stellar component to the tail, which would exist if the tail were a tidal tail. A tail comprised of only gas and young stars, with no older stellar component, is the sort of tail expected from ram pressure stripping.

Figure 3 shows that the light distribution in the inner galaxy is offset toward the SE (in the tail direction) with respect to the outer isophotes. This lopsided light distribution is consistent with ram pressure.

4.1.2. Stars and Starlike Objects Across the Face of IC3418 and a Possible Nucleus

There are several bright stars or starlike objects across the face of the main body of IC3418, concentrated within 30″ of the center of the galaxy. We give the locations, magnitudes, and colors of the seven brightest ones in Table 1, and we identify them on an *R*-band image in Figure 4. They are all spatially unresolved in our ground-based images, and for several of them, it is not possible to tell whether they are foreground stars, supergiant stars in IC3418, or star clusters in IC3418. At least one of these must be a foreground star since it is too bright to be a supergiant or globular cluster in IC3418 (S6). Some are too bright to be supergiants in IC3418 but could be either foreground stars or star clusters in IC3418 (S1, S2). Others could be any of these possibilities (S3, S4, S7).

We have a spectrum of only one of them (S5), the object closest to the galaxy center. The Keck DEIMOS spectrum shows a heliocentric velocity of 176 ± 5 km s^{-1}. The galaxy light within the slit on either side of S5 has a velocity 181 ± 5 km s^{-1}, clearly showing that it is located within the disk of IC3418. We have measured velocities of a couple of Milky Way stars in the field near IC3418, and they have velocities of −4 km s^{-1} and −25 km s^{-1}, clearly different from IC3418. S5 is unresolved spatially and spectrally, and with an absolute magnitude of $M_B = -9.35$, it is consistent with either a supergiant, a globular cluster, or a nuclear star cluster (Geha et al. 2002; Côté et al. 2006). Its color of $B - V = 0.08$ is quite blue. However, the absence of Paschen lines in the spectrum suggests that it is not a blue supergiant, implying that it is likely a star cluster.

In early type galaxies, the nuclear star cluster is almost always located at the centroid of the inner light distribution (Côté et al. 2006). S5 is not at the centroid of the inner light distribution, but the inner light distribution in IC3418 is complex, not

Table 1
Stellar Objects in or toward IC3418

Name	R.A. (J2000)	Decl. (J2000)	R_{gal}	V (mag)	$B-V$ (mag)	$V-R$ (mag)	M_V (mag)	V_{helio} (km s^{-1})	Notes
S1	12 29 45.32	11 24 20.4	0.′53	19.10	1.03	0.14	(−12.01)		FS, GC?
S2	12 29 44.55	11 24 24.5	0.′40	20.31	1.43	0.60	(−10.8)		FS, GC?
S3	12 29 44.61	11 24 13.7	0.′33	21.99	0.38	0.17	(−9.12)		FS, SG, GC?
S4	12 29 43.98	11 24 05.9	0.′17	22.29	0.81	1.13	(−8.82)		FS, SG, GC?
S5	12 29 43.31	11 24 08.9	0	21.68	0.08	0.05	−9.43	176 ± 5	Nucleus?
S6	12 29 42.58	11 24 03.5	0.′20	16.51	0.90	0.09	(−14.6)		FS
S7	12 29 42.02	11 24 02.5	0.′33	24.81	...	3.09	(−6.3)		FS, SG, GC?

Notes. Offsets measured with respect to S5, at or near the center of IC3418. Absolute magnitudes if source is in IC3418 at distance of 16.7 Mpc. Given in parentheses for foreground stars or if distance is unknown. S5 has measured velocity that puts it in IC3418. FS = foreground star in Milky Way; SG = supergiant star in IC3418; and GC = globular star cluster in IC3418.

centrally peaked, and offset from the centroid of the outer light distribution. It is close to, but offset by ∼5″ from the centroid of outer light distribution. However, given the disturbances to, and asymmetries in the galaxy, it could be the nucleus. The absolute magnitude difference of 6.8 between S5 ($M_B = -9.35$) and IC3418 ($M_B = -16.15$; Gavazzi et al. 2006) is similar to that between nuclear star clusters and their host galaxies (Côté et al. 2006). Future studies which reveal the nature of this source are of interest because the origin of nuclear star clusters are not well understood (Côté et al. 2006).

S5 is very close to the galaxy center and has a velocity close to that of the surrounding galaxy starlight. We adopt its velocity as the velocity of the galaxy, although with a larger uncertainty to allow for a modest possible offset between S5 and the mean galaxy velocity. Any offset is expected to be modest, since the rotation curves of dwarf galaxies rise very gradually. Our adopted velocity is 176 ± 15 km s^{-1}. This differs from the value of 38 km s^{-1} reported in the Goldmine database (Gavazzi et al. 2003).

Some of the star-like objects could be supergiants (S3, S4, S7). This is plausible given their high concentration near the galaxy center, but we cannot be sure as we do not have spectra of them, and they might also be foreground Milky Way stars or globular clusters in IC3418. Since supergiant stars have masses $\geqslant 10\,M_\odot$ and lifetimes $\leqslant$100 Myr, their presence would indicate some recent star formation in the central 2 kpc. This could happen even with a mean star formation quenching age of 300 Myr (Section 4.1.3), if star formation does not end uniformly in the galaxy, but some dense clouds survive the stripping of surrounding material. This is seen to happen in some stripped spiral galaxies (Crowl et al. 2005) and allows a small amount of star formation to occur after most of the gas has been stripped. This might occur especially in the galaxy center, which is the deepest part of the potential well.

4.1.3. Stellar Population Analysis of Main Body

We use our Keck LRIS optical spectra together with *Galaxy Evolution Explorer* (*GALEX*) UV colors (Martin et al. 2005; Gil de Paz et al. 2007) to analyze the stellar population of the main body of IC3418. Our Keck LRIS slit, with a width of 1″, passes through our adopted center along P.A. = 50°. We analyze eight distinct 10″ long segments of the galaxy along the major axis, extending from 0″ to 40″ on both sides of center. The location of the slit is shown on a galaxy image in Figure 4. Two sample spectra are shown in Figure 5. The optical spectra show no obvious emission lines at any location, but strong Balmer stellar absorption lines, implying a lack of ionized gas, no ongoing

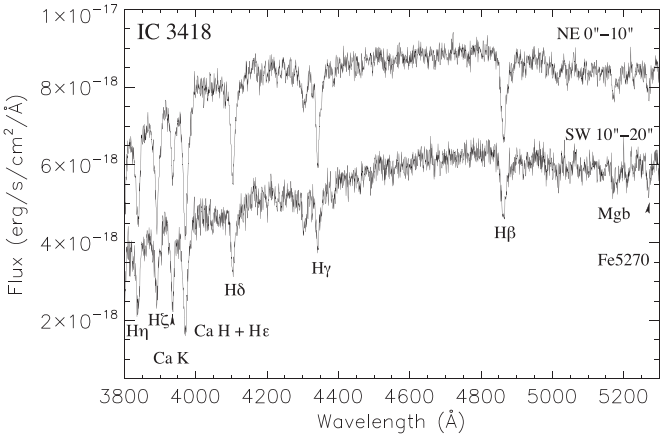

Figure 5. Keck LRIS spectrum in the blue for two regions in the main body of the galaxy. No emission lines are detected, indicating a lack of gas. The continuum is fairly blue and the Balmer lines are strong, indicating that star formation was quenched 300 ± 100 Myr ago and that a starburst occurred near the time of quenching. The two spectra shown illustrate the spatial variations in stellar properties: 0″–10″ in the NE has stronger lines and a bluer continuum than 10″–20″ in the SW. A constant offset of 2 × 10^{-18} erg s^{-1} cm^{-2} Å^{-1} has been added to the NE spectrum for display purposes.

star formation, and a post-burst stellar population, as found by Fumagalli et al. (2011).

We measure line strengths using the Lick index definitions, which uses defined pseudo-continuum bands to avoid ambiguity in setting the continuum levels. In order to constrain the star formation history in the main body of IC3418, we compare the observed line strengths and UV colors to those predicted from models generated from the Starburst99 (SB99) stellar population synthesis code (Leitherer et al. 1999). For details see Crowl & Kenney (2008).

We assume that there was constant star formation starting from a formation time (set to be 12 Gyr ago), followed by rapid quenching of star formation. We define the time since star formation ceased as the quenching time. In addition, we have considered the effect of adding a starburst at the time of quenching, in which 0%–20% of the stellar mass is formed in a burst at the time of quenching (equivalent to an increase in the star formation rate (SFR) of a factor of 1–50 for a burst duration 50 Myr). The strong Balmer lines clearly indicate a significant recent starburst. A 0% burst strength is inconsistent with all Lick indices, and the strong Hδ lines indicate a burst strength of at least 5%.

Figure 6 shows the observed strengths of several Balmer hydrogen lines versus the metal [MgFe]' Lick index as a function

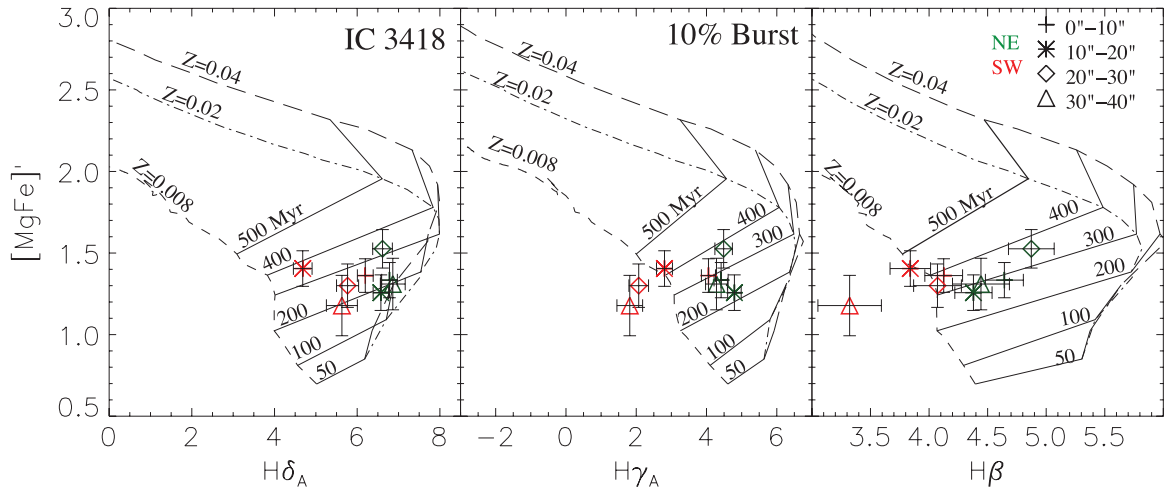

Figure 6. Lick indices and SB99 stellar population models for the main body of IC3418. Model lines are shown for a star formation history with constant star formation until a quenching time, with a starburst at quenching time which formed 10% of the stars. Dotted lines indicate stellar metallicities of $Z = 0.008$, 0.02, and 0.04 (=0.4, 1.0, and 2.0 $Z_{\odot}$). Solid lines indicate time of quenching (measured from the present time). Symbols are shown for different radial segments of galaxy. The NE side has larger line strengths than the SW side, probably due to different burst strengths. A 10% burst is the best fit to the average of the two sides.

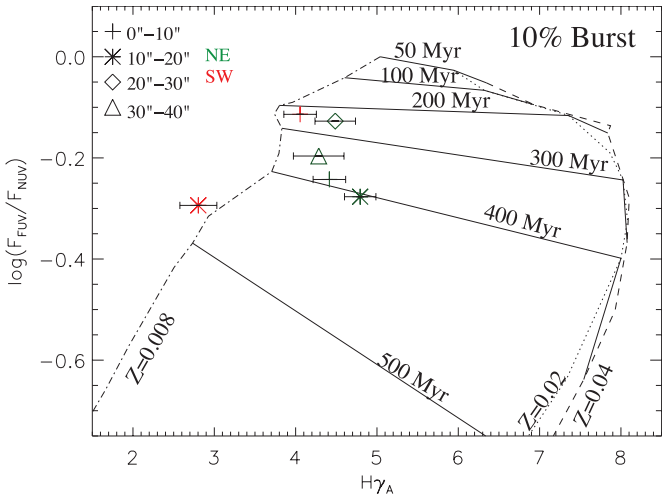

Figure 7. *GALEX* FUV/NUV flux ratios vs. the Hγ Lick index for the main body of IC3418. Model lines are shown for a star formation history with constant star formation until a quenching time, with a starburst at quenching time which formed 10% of the stars. Dotted lines indicate stellar metallicities of $Z = 0.008$, 0.02, and 0.04 (= 0.4, 1.0, and 2.0 $Z_{\odot}$). Solid lines indicate time of quenching (measured from the present time). Symbols are shown for different radial segments of galaxy. The UV flux in the outer two radial bins on the SW side was too faint to accurately measure in our small apertures. The NE side has larger line strengths than the SW side, probably due to different burst lengths.

of position. The lines in Figure 6 indicate model line strengths for various quenching times and metallicities, assuming a burst strength of 10%, which gives the best overall fit to the galaxy. Figure 7 shows the FUV–NUV colors, measured from the *GALEX* images (Martin et al. 2005; Gil de Paz et al. 2007) in apertures close in size to those used for the Lick indices, versus the strength of the Hγ line, with lines indicating the same models. Since the Lick indices and the FUV/NUV ratio have different dependencies on the burst strength, quenching time, and metallicity, using both gives more robust constraints on these parameters and also gives a measure of the uncertainties.

At a given Balmer line strength, the metal line index [MgFe]' is much weaker than would be expected for solar metallicity; thus, the stars clearly have a subsolar metallicity. Taking the average values for the three Balmer lines[9] the Lick index plots (Figure 6) show a stellar metallicity of $Z = 0.012 = 0.6 \pm 0.2\ Z_{\odot}$, with no clear evidence for a metallicity gradient.

We find a star formation quenching time of 300 ± 100 Myr, taking the average of the Lick indices for the three Balmer lines and the FUV/NUV ratio versus Hγ. This is consistent with the 200 ± 90 Myr estimated by Fumagalli et al. (2011) from the FUV/NUV ratio, although a bit older than their value perhaps because the quenching time estimate depends on both the metallicity and burst strength, which we have estimated quantitatively.

An older quenching time at larger radius is expected for ram pressure stripping, which operates from the outside in. The azimuthally averaged UV colors given in Hester et al. (2010) show a clear but modest outward gradient from FUV–NUV = 0.65 at $r = 6''$ to FUV–NUV = 1.00 at $r = 48''$. This would correspond a gradient in quenching time of $\leqslant$70 Myr from 0″ to 48″. However, neither the Lick indices in Figure 6 nor the UV ratios in Figure 7 show a clear radial gradient in quenching time. Our apertures do not show a uniform outward gradient in UV colors, and several of them have bluer colors than any of the azimuthally averaged values. This probably reflects the fact that our apertures cover localized regions with more active recent star formation. While there many be an average radial gradient in quenching time, the quenching time may not vary smoothly with position since ISM is not smooth, and localized regions of higher density can resist stripping longer than lower density regions closer to the center. These localized spatial variations in star formation histories may mask any clear radial gradient in quenching time. We adopt an upper limit on the quenching gradient of $\leqslant$70 Myr from 0″ to 48″. This is a modest gradient which implies that the galaxy was stripped quickly. In a simple model of stripping in IC3418, it takes ~150 Myr to strip gas with $\sigma = 15\ M_{\odot}\ \mathrm{pc}^{-2}$ from $r = 3$ to 0 kpc (Jáchym et al. 2013).

[9] Hβ is sometimes a less reliable indicator than the higher order Balmer lines, since the stellar absorption line is more likely to be partially filled in with residual emission from gas. Since none of the spectra show evidence for emission lines in the main body of the galaxy, we think this should be a minor effect in IC3418, so we use all three Balmer lines.

The stripping timescale in IC3418 is similar to, and perhaps quicker than this.

Much larger than any radial gradients in IC3418 are spatial differences in optical–UV colors and line strengths between the NE and SW sides. The Lick index values on SW side of the major axis are offset to lower Balmer line strengths than the NE side. Correspondingly, the optical images and $g - i$ color map shown by Fumagalli et al. (2011) show that the NE part of the galaxy is significantly bluer than the SW part. The shift in the Lick index plots is inconsistent with a difference in quenching time, and consistent with a difference in burst strength or metallicity. We regard as a difference in metallicity between the two sides as unlikely, and we think the difference is more likely attributable to a difference in burst strength. A burst strength of ∼7% of the SW side and ∼13% on the NE side would account for the difference. On small scales, variations in quenching time and burst strength are to be expected, especially in dwarf galaxies. It is unclear whether these spatial differences are related to the stripping event, as such variations might also be expected in undisturbed dwarf galaxies. A burst strength of 10% provides a good fit to the Lick indices averaged over all apertures, although the true strength of the burst could be somewhat higher or lower than 10%, as this depends on the true star formation history in IC3418, which is likely not as simple and smooth as our assumed star formation history.

In order to test the sensitivity of the quenching time and burst strength to the assumed star formation history, we have run models with alternate star formation histories. One model adopts the mean star formation history of dwarf galaxies in the ANGST sample (Figure 11 of Weisz et al. 2011), which is well approximated by an exponentially declining function with a timescale of 1.25 Gyr, plus a constant term, scaled such that 65% of the stellar mass is formed by $z = 0.7$ (6.5 Gyr ago). With such a baseline star formation history, we find fitting the Lick indices and FUV/NUV ratios in IC3418 require a very similar quenching time of 250 Myr and the same burst strength of 10%. Since there is significant variation in the star formation histories of individual dwarf galaxies and many have experienced significant bursts during their history, we have also run models with a baseline star formation history given by the lower envelope of the ANGST dIs shown in Figure 6 of Weisz et al. (2011), plus a burst at intermediate times, in addition to the recent burst at the time of truncation. In this case, fitting the Lick indices and FUV/NUV ratios in IC3418 requires a very similar quenching time of 200 Myr and a 5% burst strength at quenching time. The precise timing and strength of any burst at times earlier than 1 Gyr ago does not significantly affect the Lick indices or FUV/NUV ratios. The baseline star formation history in this case has a relatively low SFR over most of the galaxy's history, and a large amount of star formation (∼30% of the total stellar mass) in the last 1 Gyr. Thus, the only way to have a burst strength much lower than ∼10% at quenching time is to have another large recent burst in the last ∼1 Gyr. Even in this extreme case, the burst required at quenching time is ∼5%. In summary, the precise timing and strength of the recent starburst depend only a little on the assumed star formation history before ∼1 Gyr ago, and even with these alternate star formation histories, the quenching time and burst strength fit within the adopted values of 300 ± 100 Myr and 10% ± 5%.

Other ram pressure stripped galaxies are observed to experience, or have experienced, starbursts at the time of stripping (Crowl & Kenney 2006; Abramson et al. 2011; Merluzzi et al. 2013). A spiral galaxy experiencing ram pressure stripping in the rich cluster A3558 has an ongoing starburst over part of the disk with a five times increase in the SFR over the past 100 Myr, plausibly triggered by ram pressure (Merluzzi et al. 2013). Among the Virgo spiral galaxies studied spectroscopically by Crowl & Kenney (2008), the one with spectral properties most similar to IC3418 is NGC 4522, a spiral with clear evidence for ongoing ram pressure stripping. The gas-stripped outer disk of NGC 4522 has the strongest Balmer lines of all the Virgo spirals studied by Crowl & Kenney (2008), as it was stripped most recently (100 Myr ago) and had a starburst at the time of truncation. The NGC 4522 starburst formed 2% of the stellar mass, corresponding to a five times increase in the SFR over 100 Myr, the same intensity as the starburst in the A3558 spiral (Crowl & Kenney 2006). IC3418 has even stronger Balmer lines than NGC 4522, but redder FUV–NUV colors, suggesting an older quenching time but a stronger burst, with an amplitude of ∼10% of the stellar mass. This may be because star formation is generally burstier in dwarfs than spirals but might also be due a more extreme ram pressure event in this fully stripped dwarf.

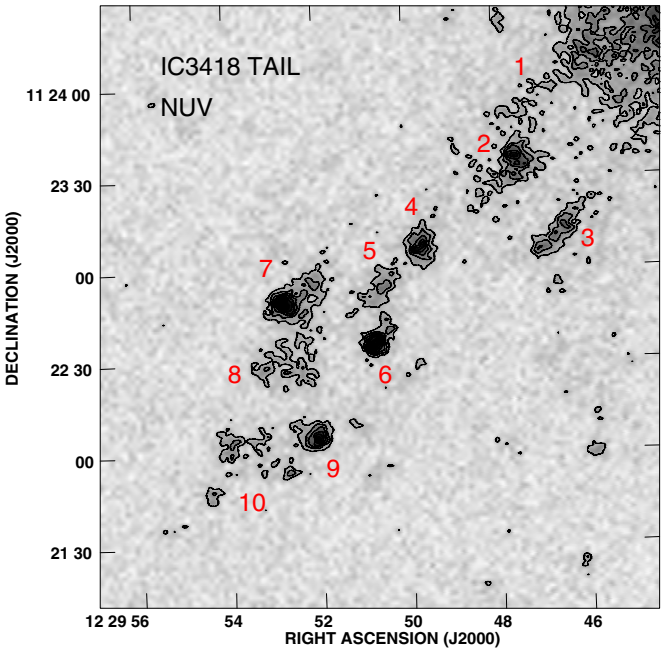

Figure 8. *GALEX* NUV grayscale and contour image of tail of IC3418, with distinct regions numbered. Eight of the ten UV regions are elongated with position angles similar to the large scale tail.

(A color version of this figure is available in the online journal.)

4.2. Tail of IC3418

4.2.1. Tail Morphology in UV, Optical, and Hα

GALEX UV images of IC3418 (Chung et al. 2009; Hester et al. 2010; Fumagalli et al. 2011) show a remarkable one-sided tail of young stars extending 17 kpc outward from the main body of the galaxy (Figure 1). At the *GALEX* resolution of $6'' = 0.46$ kpc, there are ∼10 distinct bright UV sources within the tail, with morphologies of diffuse regions, knots, linear streams, or head–tail sources, which are a combination of knots and linear streams. While Hester et al. (2010) and Fumagalli et al. (2011) have previously described the tail, we point out several key features of the tail morphology not described by them. In Figure 8, we label 10 UV tail features, numbered sequentially with increasing distance from galaxy. Our labeling is different from and simpler than both Hester et al. (2010)

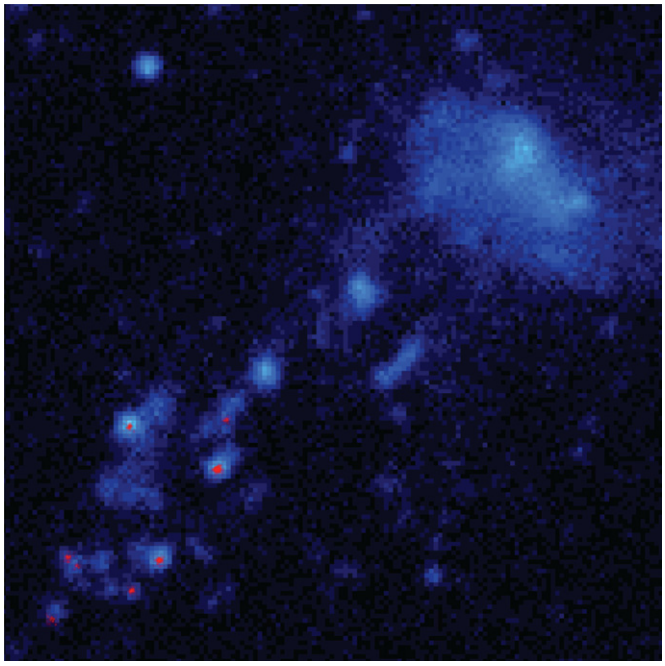

Figure 9. Hα+[N II] (red) plus NUV (blue) image of IC3418, showing that all bright H II regions are in the outer part of the tail.

(A color version of this figure is available in the online journal.)

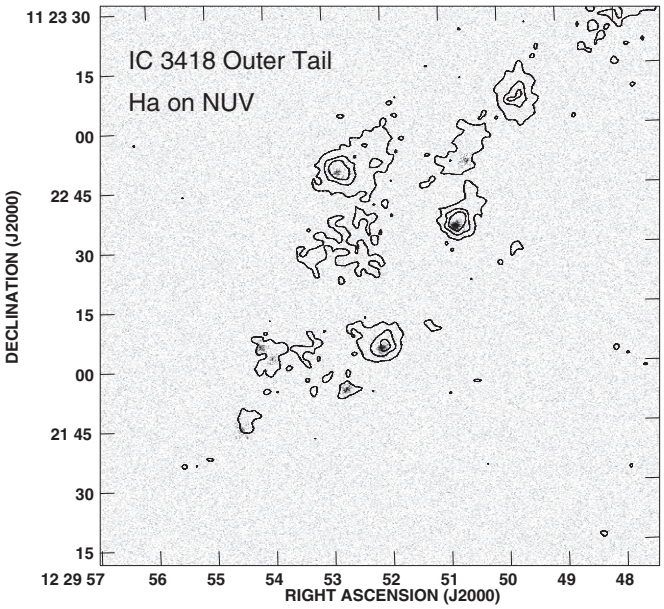

Figure 10. Hα+[N II] line image on NUV contours of outer tail, showing H II regions. Note bright H II regions at heads of head–tail UV sources, and the outward offset of the H II regions relative to the UV peaks.

and Fumagalli et al. (2011). We do not create separate lists for "knots" and "filaments" or "diffuse regions," since there is overlap and some sources show characteristics of more than one morphology. For example, UV7 has a head–tail morphology (discussed below). Fumagalli et al. (2011) label the head as K5 and the tail as F2, whereas we label it as one source, since we think that better reflects its nature.

The seven brightest UV tail features are elongated and nearly parallel to each other, with position angles 125°–138°, which matches the P.A. of the large-scale tail, 132° ± 1°. The longest stellar stream is 25″ ≃ 2 kpc in length. An eighth feature, UV1, the UV tail stream closest to the galaxy, has a P.A. offset by ≃10° from the others. This feature, which was not identified by Hester et al. (2010) or Fumagalli et al. (2011), is faint and has redder UV colors, it appears slightly curved, and may be an "older" stellar stream now falling back into galaxy.

WIYN images show optical counterparts for all the UV sources, although as seen in Figure 1, the tail sources stand out from the background galaxies much more in the UV than the optical, indicating recent star formation. The structure of the stellar streams contain information on the numbers and sizes and motions of dense clumps of star-forming gas, and the length of stellar streams contain information on how long dense gas lumps retain an identity. Within the kpc-scale NUV sources, the higher resolution optical images reveal complexes of optical knots with characteristic lengths of 0.5–3 kpc and widths of 200–400 pc, rather than simple monolithic streams. The optical substructure suggests multiple centers of star formation within outwardly accelerating 200–400 pc diameter gas concentrations.

The only Hα emission detected in the imaging is from discrete H II regions in the outer half of the tail, at distances ranging from 10 to 17 kpc from the galaxy center. These regions are faint, and at this level, the continuum-subtracted image also shows artifacts from bright continuum sources. We have individually examined all features from the continuum-subtracted image, in both the broad and narrowband filter images to learn which features are real Hα sources. Based on the ratio of counts in the broad and narrowband filter images, we identify only eight "true" H II regions, which are the same ones shown by Fumagalli et al. (2011). We masked out everything but the confirmed H II regions to make the Hα–NUV overlays in Figures 9 and 10. Fluxes of all H II regions are given in Table 2. The total Hα+[N II] flux of all the tail H II regions is 3.0×10^{-15} erg s^{-1} cm^{-2}. This total flux is consistent with Fumagalli et al. (2011); although, we find significantly different fluxes for some of the individual H II regions.

Spectroscopy has revealed three faint emission line sources not detected in the imaging, including two in the inner tail, located within UV3 at ∼6 kpc from the galaxy center, and one in UV9, a few arcseconds closer to the galaxy than the bright H II region detected in UV9. These are approximately an order of magnitude fainter than the faintest H II regions detected in the imaging and are likely associated with older and less massive stars. They have Hα luminosities of $\sim 10^{35}$ erg s^{-1}, and at least the two brighter ones (which have more than two lines detected) have line ratios similar to those of H II regions in the outer tail, with Hα ≫ [N II] (see Figure 13). With such luminosities and line ratios, these emission line sources could be classical H II regions, powered by single B stars photoionizing the surrounding gas remaining from the birth cloud, or single Be stars, which photoionize gas ejected from the star, or planetary nebulae. B2–B4 stars have main-sequence lifetimes of 30–100 Myr, and the stars producing planetary nebulae are generally even older. Thus, the low-luminosity emission line sources in the inner tail are consistent with recent but not ongoing star formation.

The overlays of the Hα and NUV images in Figures 9 and 10 shows that all Hα sources are coincident with NUV sources. Three of the brightest H II regions are located at the heads of UV head–tail sources, with tails pointing back toward the galaxy (UV6, UV7, and UV9). Figure 10 shows that the Hα and UV peaks are offset, with the Hα located 1″–2″ = 80–150 pc further from the galaxy than the UV peak. UV6 and UV7 exhibit clear head–tail morphologies; in UV9, which is the outermost bright

Table 2
Tail H II Regions in IC3418

Name	R.A. (J2000)	Decl. (J2000)	R_{gal}	Hα+[N II] Flux (10^{-17} erg s^{-1} cm^{-2})	V_{helio} (km s^{-1})	Notes
UV3-Hα1	12 29 46.70	11 23 08.3	1.′33	∼3	236	a
UV3-Hα2	12 29 46.98	11 23 04.7	1.′42	∼1	253	a
UV5-Hα1	12 29 50.60	11 22 50.8	2.′17	16	218	F3
UV6-Hα1	12 29 50.82	11 22 35.0	2.′40	123	220	K6
UV7-Hα1	12 29 52.77	11 22 48.9	2.′62	20	293	K5
UV9-Hα1	12 29 52.11	11 22 04.6	2.′98	70	225	K4
UV9-Hα2	12 29 51.98	11 22 06.1	2.′93	∼2	226	a
UV10-Hα1	12 29 52.76	11 21 54.2	3.′22	30	221	K2
UV10-Hα2	12 29 54.19	11 22 05.4	3.′33	24	...	b, K3-NE
UV10-Hα3	12 29 54.00	11 22 02.6	3.′33	10	254	K3-SW
UV10-Hα4	12 29 54.55	11 21 44.8	3.′63	10	273	K1

Notes. Names of sources in Fumagalli et al. (2011), for those sources detected by them. (a) For H II regions detected only by spectroscopy, an approximate Hα flux has been estimated by scaling the peak line intensity to those of sources detected in both imaging and spectroscopy. Accuracy is a factor of ∼2. These faint emission line sources are likely powered by single B stars, or are planetary nebulae. (b) UV10-Hα2 has no velocity since it was not covered by the spectroscopy.

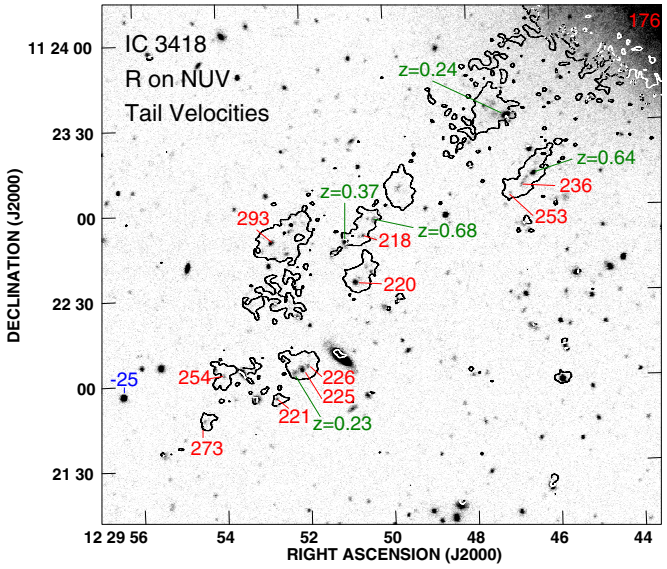

Figure 11. Velocities of sources in the tail region of IC3418 plotted on *R*-band grayscale image with contours of NUV emission. Red indicates heliocentric velocities (in km s^{-1}) of emission line sources (H II regions) in the tail of IC3418, blue indicates velocities of foreground stars, green indicates redshifts of background galaxies.

(A color version of this figure is available in the online journal.)

Ha/NUV source, the NUV "tail" is very short, but there is a clear offset between the Hα and NUV peaks in the same direction as the tails. This is evidence for gas preferentially accelerated and dynamically decoupled from newly formed stars (Hester et al. 2010).

Correcting for the presence of contaminating background galaxies shows that possibly four of the outer tail H II regions are located near the heads of UV streams, with an outward offset (UV5 as well as UV6, UV7, and UV9). The innermost H II region in the outer tail is located 130″ = 10 kpc from the nucleus, near the middle of a linear NUV feature (UV5). However Figure 11 shows that background galaxies form the outermost and innermost parts of UV5. Removing them would likely put the H II region in UV5 near the head of a stellar stream. Similarly, the outermost part of UV9 coincides with a background galaxy, so the portion of UV9 that is associated with IC3418 has an even clearer head–tail morphology than suggested by Figure 10.

Not all of the H II regions are at the heads of head–tail features. Four H II regions are in the outermost part of tail, beyond the brightest UV sources, in a triangle-shaped feature of lower surface brightness UV emission (UV10). The outermost Hα and UV source detected is at the tip of this triangle, 218″ = 17 kpc from the nucleus. These outermost four H II regions are faint in both Hα and NUV, so the outer tail has modest active star formation and not much stellar mass formed.

Of the six brightest NUV sources in the tail, the outer three all have Hα, and the inner three have little or no Hα. These observations suggests three distinct zones in the tail, with different Hα/UV ratios: the inner tail (inner 2′; UV1–4) has bright UV but little or no Hα, with an Hα/NUV ratio <10% that of the outer tail, the outer tail (2′–3′, UV5–9) has bright UV and modest Hα, and the very outer tail (3′–4′, UV10) has fainter UV and modest Hα, with an Hα/NUV ratio 1.6 times that of the outer tail. The inner tail UV sources show no obvious systematic difference from the outer (middle) tail UV sources in UV or optical color, whereas the very outer tail features have bluer colors (Fumagalli et al. 2011).

The morphologies of the tail features differ in the three zones. The inner tail has UV-bright linear streams and knots, but no head–tail features and very little Hα emission. The outer tail has UV-bright head–tail features, i.e., knots with Hα at the heads of linear stellar streams ("fireballs"). The very outer tail has lower surface brightness diffuse UV features with associated Hα emission. We propose the following interpretation for the different tail zones. Nearly all the gas has been stripped from the inner tail, and some stellar features here may be falling back into the galaxy. The outer tail still has gas and ongoing star formation, with some large gas concentrations being outwardly accelerated, forming fireballs. The very outer tail still has gas and ongoing star formation, but it has smaller gas concentrations and therefore less bright stellar knots. Part of this is likely due to the spatial segregation of gas clumps of varying densities—at a given ram pressure, lower density clumps are accelerated more and get further from the galaxy (Tonnesen & Bryan 2010, 2012; Jáchym et al. 2013). This could help explain the difference between the outer and very outer tail.

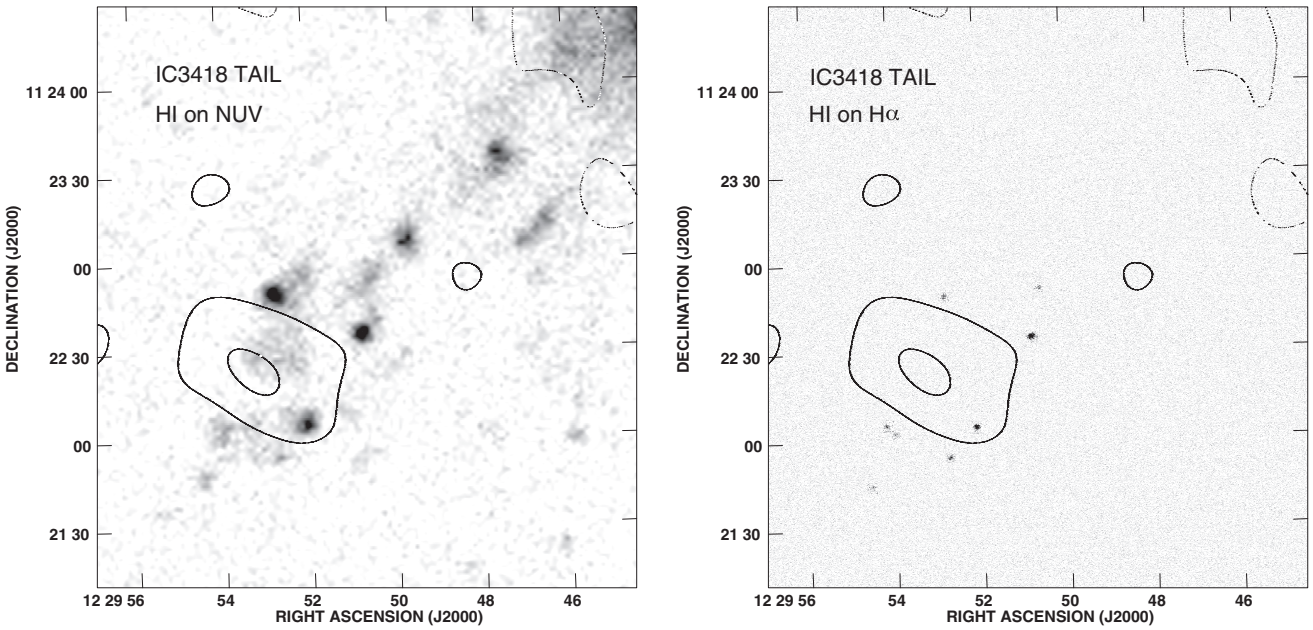

Figure 12. Map of H I channel centered at 234 km s^{-1} with width of 10 km s^{-1} overlain on (left) NUV image and (right) Hα image of IC3418. Contour levels are $-2\sigma, 2\sigma, 4\sigma$, where $1\sigma = 0.6$ mJy beam^{-1} $= 0.06\ M_\odot$ pc^{-2} $= 8 \times 10^{18}$ cm^{-2}.

Some features of the UV–Hα morphology in IC3418 are like those in the "Fireball Galaxy" RB199 in the Coma cluster, in which UV-bright stellar streams in the outer part of its tail have associated Hα emission, but those closer to the galaxy center are seen only in the UV (Yoshida et al. 2008).

The width of the tail in IC3418 is relatively constant with radius. Simulations without radiative cooling show flaring of the tail (Roediger & Brüggen 2008), whereas those with cooling show narrower tails with nearly constant width (Tonnesen & Bryan 2010). The presence of star formation in the tail is a clear signpost of cooling, and thus, is likely related to the narrow width of the tail. The tail width of $45'' = 3.5$ kpc is similar to the lateral extent of the region in the main body of the galaxy showing evidence of recent star formation. This may explain the tail width—it has roughly the same lateral extent as the part of the galaxy that was most recently gas-stripped.

Deeper observations should show evidence of tail/halo stars further out from the centroid of the tail than the bright UV features, reflecting stars formed from gas stripped from the galaxy's outer disk. Such stars would have fallen back more toward the galaxy. Stream UV1 may be such an example—its stars are older, the stream is furthest from the tail midline, and it is the most curved stellar stream. It could be a stream formed from gas further from the galaxy center, stripped at an earlier time.

The Hα luminosity of the H II regions in the tail corresponds to a SFR of $1.9 \times 10^{-3}\ M_\odot$ yr^{-1}. This is a small amount. Fumagalli et al. (2011) estimated the mass of newly formed stars in the tail to be $\sim 2.5 \times 10^6\ M_\odot$ over $\sim$200 Myr, from fits to the UV–optical spectral energy distributions (SEDs). This is less than 1% of the galaxy's stellar mass and suggests that stars formed in ram pressure stripped tails do not make a large contribution to the intracluster stellar population in Virgo. Indeed, most of the gas stripped from Virgo spirals remains gas and joins the ICM (Vollmer et al. 2012).

4.2.2. H I in the Tail of IC3418

We have detected weak H I emission in the outer tail from the VIVA data (Chung et al. 2009). While we originally reported no H I emission in IC3418 (Chung et al. 2009), we reinspected the VIVA data cube and carefully examined those portions of the cube which matched the positions and velocities of the H II regions in the tail. When we spatially smooth the cube to a resolution of 30″, we find emission in one 10 km s^{-1} width channel with a peak intensity of 4σ, where the rms is 0.6 mJy beam^{-1}. This weak but statistically significant H I feature peaks at a velocity of 234 km s^{-1} and has an H I flux of 0.038 ± 0.007 Jy km s^{-1}.

An overlay in Figure 12 of the H I channel at 234 km s^{-1} on the NUV and Hα images show that the H I emission is located in the outer part of the tail and is extended in the direction perpendicular to the tail. The H I peak is centered closest to diffuse region UV8 and covers the UV/Hα head–tail source, UV9. It is located just beyond the bright UV/Hα head–tail sources, UV6 and UV7, and lies just inside the outermost source UV10 and its H II regions. While many of the tail H II regions are slightly beyond the region where H I has been detected, it is likely that the detected H I is merely the peak of a more extended H I distribution which covers the H II regions. The H I velocity of 234 ± 5 km s^{-1} is generally consistent with the H II regions in the tail and is very close to that of UV9, which has $v =$ 225–226 km s^{-1} (as discussed below).

The detected flux corresponds to $3.7 \times 10^7\ M_\odot$, which is only $\sim$6% of the expected H I mass of a typical dI with the mass of IC3418 (Gavazzi et al. 2005). Most of the stripped gas must be more spread out or in another phase.

Our reinspection of the H I data cube, involving smoothing with different combinations of spatial and velocity averaging, still shows no H I in the main body of galaxy, and we place an upper limit similar to that reported in Chung et al. (2009), of $6 \times 10^6\ M_\odot$ of H I (3σ) assuming a 100 km s^{-1} profile per 20″ beam. The velocity range of the galaxy is now better known than at the time of the original VIVA analysis, when the reported velocity of 38 km s^{-1} from the GOLDMINE database (Gavazzi et al. 2003) was very close to Galactic H I emission. The velocity range of the galaxy and tail is now known to be 140–290 km s^{-1}, outside the range of Galactic H I. Thus, our upper limit is now more reliable as the VIVA H I data cube has good data over the

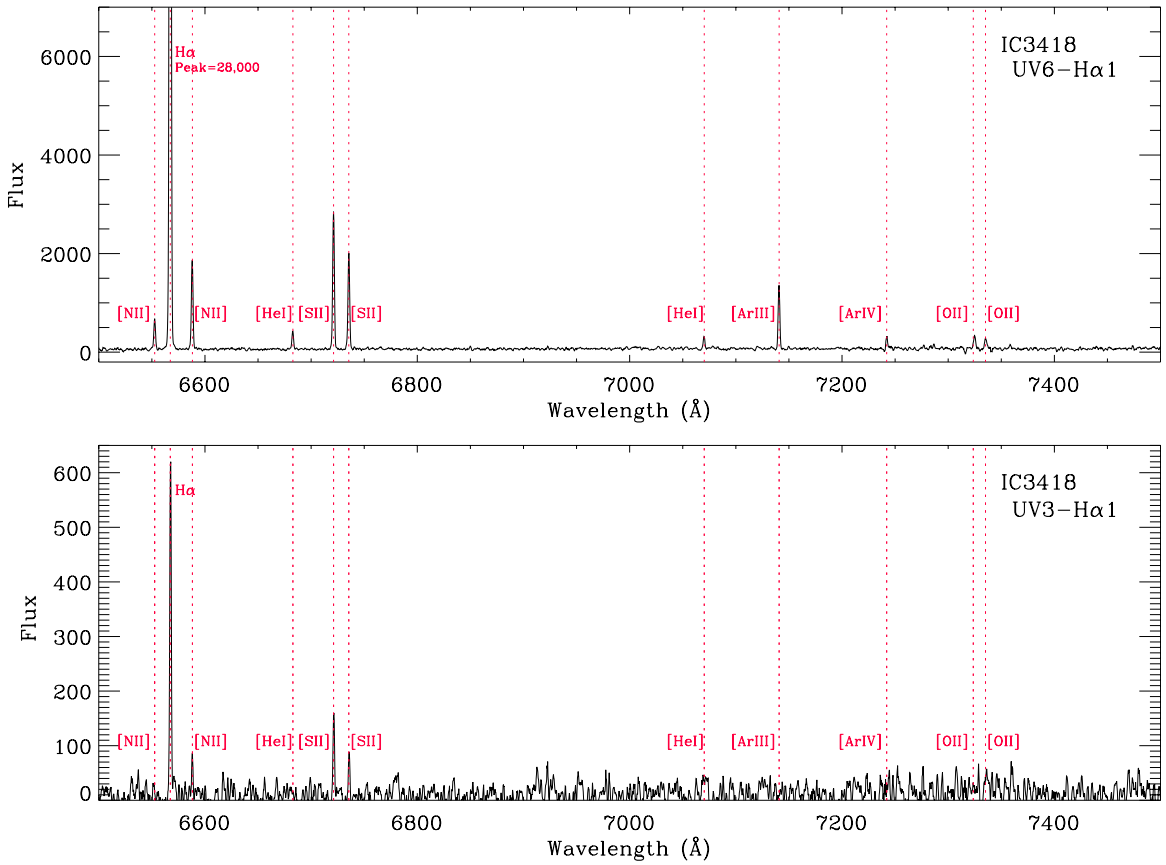

Figure 13. Keck DEIMOS spectra of two of the H II regions in the tail of IC3418, with lines identified. The upper panel shows the strongest H II region UV6-Hα1, and the lower panel shows one of the faintest H II regions, UV3-Hα1, from the inner tail. The flux scale is in arbitrary units.
(A color version of this figure is available in the online journal.)

entire velocity range of IC 3418. With this upper limit, the main body of IC3418 has less than 1% of its expected H I mass.

4.2.3. Kinematics of Tail Sources in IC3418

With the Keck DEIMOS spectroscopy, we have detected emission lines from every targeted H II region seen in the imaging, plus weak emission lines in the UV feature (UV3) near the galaxy which was undetected in the Hα imaging. We have also detected emission + absorption line spectra from several background galaxies in the tail region. The brightest optical sources within U2, U3, and U5 are all background galaxies with $z = 0.23$–0.68. We discuss in Section 4.2.5 how this may affect the optical–UV SEDs and resultant "ages" of tail sources derived by Fumagalli et al. (2011). The velocities of the H II regions and the redshifts of the background galaxies are indicated in Figure 11.

Figure 13 shows spectra for two of the H II regions. Multiple lines are detected for all H II regions, with line ratios characteristic of H II regions with subsolar metallicity. The [N II]λ6583/Hα ratios range from 0.06 to 0.12, which correspond to 12+log(O/H) ratios of 8.22–8.38, or 0.36–0.53 $Z_{\odot}$ (within a factor of 2.5), according to Pettini & Pagel (2004). Thus, the gas in tail has a metallicity similar to the stars in the main body.

The velocities of tail H II regions are shown in a position–velocity diagram in Figure 14. The velocities of all tail H II regions (218–293 km s^{-1}) are redshifted with respect to the main body of galaxy ($V = 176$ km s^{-1}). This is consistent with acceleration by ram pressure, since the tail sources

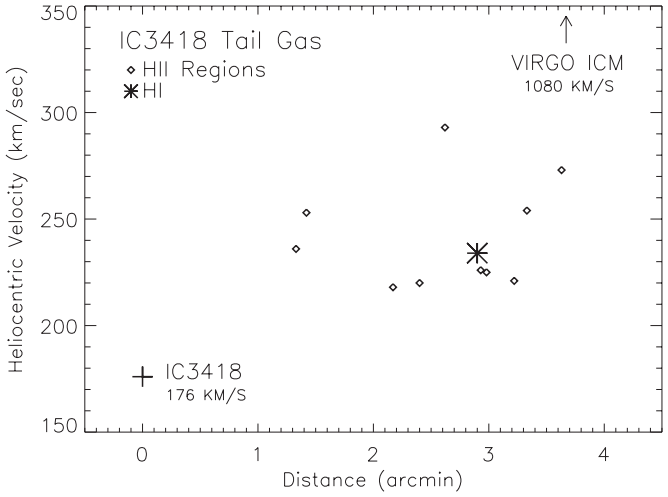

Figure 14. Position–velocity diagram for gas in tail of IC3418. Velocities of H II regions and the H I cloud plotted vs. distance from the center of IC3418.

have velocities which are offset toward the cluster velocity. An inspection of Figure 14 shows that a velocity gradient can be fit from the central velocity of IC3418 through the tail H II regions, but random motions are comparable in amplitude to any gradient. A large range in the velocities of young tail stars is also seen in simulations of ram pressure stripped tails (Tonnesen & Bryan 2012), presumably reflecting the fact that clouds with different initial gas surface densities will experience different accelerations. The simulations also show a clear gradient in velocities,

but the tail in IC3418 may not be long enough (and extend to high enough velocities) to show such a clear gradient. The tail kinematics should also reflect the disk kinematics. A lateral gradient across the tail is expected from the disk rotational motion and has been observed in the tail star clusters of the stripped spiral galaxy ESO 137-001 (Sun et al. 2010). There is no clear lateral gradient among the tail H II regions in IC3418, probably because the rotation curve is shallow in dwarf galaxies, and the velocity variations are dominated by other factors.

The tail H II regions have velocities which are low relative to the galaxy, and much closer to the galaxy ($v = 176$ km s^{-1}) than the cluster ICM ($V = 1080$ km s^{-1}). This helps explain the fireballs, i.e., H II regions at heads of linear UV-bright stellar streams. Since the velocities of the tail H II regions are still very different from that of the cluster ICM, they are probably still experiencing strong ram pressure from the cluster ICM, and strong gas acceleration from ram pressure is required to cause the observed spatial offsets between the gas and stars in the fireballs.

The simulations of Tonnesen & Bryan (2012) predict stripped gas tails with a large range of velocities at any distance, due to differential stripping and acceleration. These simulations show that some gas extends to the cluster velocity; but, even after a few hundred Myr of stripping, most of the gas is at velocities less than the cluster velocity and much of the gas has velocities one-third to one half of the way to the cluster velocity. However, the tail H II regions in IC3418 extend kinematically much less than this, only 15% of the way to the cluster velocity. Thus, either the gas tail is much longer and young stars exist only in the inner part, or the tail is dynamically young and no part of it has had sufficient time to be accelerated closer to the cluster velocity. The former is more likely in IC3148, given the absence of gas in the main body which indicates a relatively advanced evolutionary stripping state.

The low velocities also imply that while some of the tail sources will likely escape and add to the intracluster stellar population, others will likely fall back into the galaxy and add to the galaxy's halo. Assuming the mass model of IC3418 described by (Jáchym et al. 2013), which has a total mass of $7.5 \times 10^9\ M_\odot$, the escape speed is $\sim$110 km s^{-1} at $r = 5$ kpc, which is the projected distance of the inner tail, and is $\sim$60 km s^{-1} at $r = 17$ kpc, which is the projected distance of the outermost tail. Because of projection effects, the tail sources have higher galactocentric distances than the projected ones and therefore lower escape speeds, and also have higher galactocentric (three-dimensional, 3D) velocities. H II regions in the inner tail have line-of-sight velocities which differ from the main galaxy by 40–75 km s^{-1}, and the 3D velocities are probably $\sqrt{2}$ higher, or 55–105 km s^{-1}. Some of these velocities are less than the local escape speed of $\sim$100 km s^{-1}, meaning that some of the inner tail features are likely to fall back into the galaxy. However, some of the H II regions in the outer tail have line-of-sight velocities which differ from the main galaxy by 95–115 km s^{-1}, and the 3D velocities are probably $\sqrt{2}$ higher, or 135–160 km s^{-1}. Even their projected velocities exceed the local escape speed of $\sim$60 km s^{-1}, meaning these sources are definitely unbound and will escape into intracluster space.

A recent paper by Ohyama & Hota (2013) presents spectroscopy of an emission line star in the direction of the tail and suggests that it is a supergiant located within the tail. The velocity of this star is -99 km s^{-1}, which is inconsistent with the velocities of the H I and H II regions detected in the tail, which range from 218–293 km s^{-1}. It remains unclear whether this star is physically associated with IC3418 or is instead a foreground Milky Way star.

4.2.4. Acceleration Timescales for Tail Sources

We can relate the tail length and velocities to the timescale for accelerating the gas parcels which are forming stars in the tail. The line-of-sight and sky components of velocity and distance of a tail source with respect to the main galaxy, are related by

$$\begin{aligned} L_{\rm tail}({\rm los}) &= f\ v_{\rm tail}({\rm los})\, t \\ L_{\rm tail}({\rm sky}) &= f\ v_{\rm tail}({\rm sky})\, t, \end{aligned} \tag{1}$$

where $L_{\rm tail}$(sky) is the distance traveled in the plane of the sky, $L_{\rm tail}$(los) is the distance traveled along the line of sight, $v_{\rm tail}$(sky) is the current velocity in the plane of the sky, $v_{\rm tail}$(los) is the current velocity along the line of sight, t is the time of acceleration, and f is a fraction that depends on the acceleration profile and is a measure of the time-averaged acceleration.

If a cloud starts with zero velocity and the acceleration is constant, $f = 1/2$. There are three reasons why the acceleration is not constant. First, the acceleration is due to the fight between ram pressure and gravity, and the gravitational restoring force depends on the initial gas position in the galaxy and decreases as the gas moves away from the galaxy. Second, the ram pressure $\rho(v_{\rm gas} - v_{\rm ICM})^2$ on stripped clouds drops as they become accelerated away from the galaxy velocity toward the ICM velocity $v_{\rm ICM}$. This is a small effect for the tail sources in IC3418 since they have velocities much closer to their original (galaxy) velocities than the ICM velocity. Moreover, the first and second effects act in opposite directions, so they partly offset each other. Third, the ram pressure on the galaxy varies strongly with time as the galaxy orbits through the cluster. Simulations of orbiting galaxies by Jáchym et al. (2013) suggest that it can change by a factor of two over 200 Myr timescales. We do not know whether the ram pressure is currently increasing or decreasing, so we adopt $f = 1/2$ corresponding to constant acceleration and recognize the uncertainty is a factor of $\sim$2.

If we adopt $f = 1/2$ and 300 Myr for the acceleration time of the outermost tail sources, from the star formation quenching time in the main body, then $v_{\rm tail}({\rm sky}) = 2\ L_{\rm tail}({\rm sky})/t = 2$ (17 kpc)/300 Myr = 113 km s^{-1} and $v_{\rm tail}({\rm sky}) = 1.13\ v_{\rm tail}({\rm los})$. The tail length along the line of sight would be $L_{\rm tail}({\rm los}) = f\ v_{\rm tail}({\rm los})\ t = 1/2$ (100 km s^{-1}) (300 Myr) = 15 kpc, and the tail 3D length is 23 kpc. We can also use this to estimate the sky velocity of IC3418, $v_{\rm gal}({\rm sky}) = 1.13\ v_{\rm gal}({\rm los}) = 1.13(900$ km s$^{-1}) = 1000$ km s^{-1}, since for small acceleration $v_{\rm tail}({\rm sky})/v_{\rm tail}({\rm los}) \simeq v_{\rm gal}({\rm sky})/v_{\rm gal}({\rm los})$. Thus, it is likely that the sky and line of sight components of motion for IC3418 are similar.[10]

On the other hand, we can use these relationships to provide an independent measure of the quenching time, by requiring that the velocity of IC3418 is within a reasonable range. In order for IC3418 to have a 3D velocity less than 2000 km s^{-1}, which is the approximate maximum of any Virgo galaxy, $v_{\rm gal}({\rm sky}) < 1800$ km s^{-1}, which corresponds to $t > 200$ Myr.

[10] It may be possible in the future to estimate one of the unknowns, $L_{\rm tail}$(los) or $v_{\rm tail}$(sky), if the other becomes known, without knowing either f and t by eliminating t from Equation (1). We have $L_{\rm tail}({\rm sky}) \times v_{\rm tail}({\rm los}) = L_{\rm tail}({\rm los}) * v_{\rm tail}({\rm sky}) = 1700$ kpc km s^{-1}, since we know $L_{\rm tail}({\rm sky}) = 17$ kpc and $v_{\rm tail}({\rm los}) = 100$ km s^{-1} for the outermost tail H II regions. While we do not know $L_{\rm tail}$(los) or $v_{\rm tail}$(sky) individually, we know the product $L_{\rm tail}({\rm los}) \times v_{\rm tail}({\rm sky}) = 1700$ kpc km s^{-1}.

Table 3
Background Galaxies in Direction of IC3418's Tail

Name	R.A. (J2000)	Decl. (J2000)	R_{gal}	R (mag)	z	Notes
G1	12 29 47.04	11 23 31.8	1.′10	20.53	0.24	SDSS J122947.04+112332.3
G2	12 29 46.41	11 23 11.2	1.′22	21.59	0.64	SDSS J122946.45+112311.8
G3	12 29 50.27	11 22 56.8	2.′08	22.75	0.68	
G4	12 29 50.97	11 22 48.3	2.′31	21.58	0.37	
G5	12 29 52.22	11 22 03.3	3.′02	22.33	0.23	

Notes. Offsets (R_{gal}) measured with respect to S5, at or near the center of IC3418.

This agrees well with the quenching time measured from the stellar population in the main body and serves as an independent measure of it. If the acceleration time were as short as 100 Myr, this would imply $v_{gal}(sky) = 3000$ km s^{-1}, which is unreasonably high.

4.2.5. Ages of Stellar Features in Tail

The stellar features in the tail exhibit a range of UV–optical colors. There appears to be an overall color gradient in the tail, with the outermost tail sources being the bluest and youngest (Fumagalli et al. 2011). There is also significant scatter about this mean radial trend in color. Part of this is likely due to the inclusion of contaminating background galaxies (and possibly foreground stars), and part of it may be intrinsic.

Fumagalli et al. (2011) estimated the ages of the tail stellar features from UV–optical SEDs and found a large age range from 80 to 1400 Myr. Such a large range would suggest a surprisingly long period of strong ram pressure stripping, and it even calls into question a ram pressure stripping origin for the stellar features in the tail, since some of the proposed ages are much older than the quenching time in the disk of 200–400 Myr. Such old stars in the tail would require that some gas was stripped from the galaxy long before most of the gas was stripped—either the outer disk gas was stripped long (∼1 Gyr) before the inner disk, or lower density gas from the inner disk was selectively stripped, decoupling from denser gas which was not stripped for another ∼1 Gyr. The long timescales for both scenarios are problematic. Orbital times in the cluster are ∼2–3 Gyr, during which ram pressure is expected to vary by 1–2 orders of magnitude, depending on the orbit. Simulations show that most stripping occurs when the ram pressure increases significantly during the period of radial infall, which is an interval that generally lasts less than a few hundred Myr (Vollmer et al. 2001), much less than the 1.4 Gyr required from the stellar age estimates.

Alternatively, it may be that some of the ages are overestimates. We note that the Fumagalli et al. (2011) photometry was measured in 6″ apertures, to match the *GALEX* resolution. At this resolution, background and foreground sources could be important, especially in the optical. Whereas in the UV the tail sources are much brighter than anything in the background, in the optical, the tail sources are hard to pick out among the many background sources (Figure 1). Spectroscopy of tail sources from Keck shows that this is indeed a problem. Background galaxies, with redshifts between $z = 0.23$ and 0.68, are confirmed to exist in some of the tail filaments. Their locations are shown in Figure 11 and given in Table 3. Fumagalli et al. (2011) estimated ages of 600–1400 Myr for 5 of their 12 tail sources. Of these, three (F3, F4, K4) have confirmed background galaxies, and in two of them (F3 and F4), the galaxy is the brightest optical source. Inclusion of these bright optical background sources in a UV–optical SED will clearly result in an overestimate of the stellar age. Other tail features may also include background galaxies, but we did not position slits on many of the knots. Seven of the twelve tail sources studied by Fumagalli et al. (2011) have age estimates of 80–390 Myr, which seems reasonable given the quenching time in the galaxy, and we suspect that all the tail sources have ages within this range. Sorting out the true age distribution in the tail will require a more complete identification of true and contaminating tail sources.

While some of the color variation in tail sources is due to contaminating sources, some intrinsic local variation in age may be expected in the tail. In adaptive mesh refinement (AMR) simulations, Tonnesen & Bryan (2012) find that disk gas with a range of densities (although not dense clouds) is stripped continuously, so there is a range of gas densities throughout the tail. Accordingly, the time it takes for radiative cooling and possibly compression by the ICM, and consequent star formation to occur, also varies throughout the tail. Thus at any one time, the tail may have dense gas and star formation over a large radial range. Moreover, with an extended period of gas stripping, in the inner tail, it is possible to have outwardly moving young stars at the same distance as older backfalling stars. In the case of IC3418, which is now (almost) completely gas-stripped, there is no more gas from the galaxy to supply to the tail, and the gas in the tail has moved further downstream. This may explain why the only bright H II regions and the bluest stellar features are in the outer half of the tail.

4.3. Gas Content of the Main Body and Tail

The main body of the galaxy is very gas poor as H I, Hα, and X-ray emission are undetected (Hoffman et al. 1989; Chung et al. 2009; Jáchym et al. 2013). There is a marginal detection of CO in the central few arcseconds of galaxy, corresponding to a gas mass of $\sim 10^6\ M_\odot$, with the standard CO–H_2 relation (Jáchym et al. 2013). Even if this is a real detection, the amount of gas is very small. IC3418 is H I-deficient and H_2-deficient compared to star-forming dwarfs (Jáchym et al. 2013), with less than 1% of the expected H I+H_2 mass. Virtually all the gas has been stripped from its main body.

The only gas clearly detected in IC3418 is in the tail. In addition to the H II regions, there is $3.7 \times 10^7\ M_\odot$ of H I. CO is undetected in the tail with an upper limit which corresponds to an H_2 mass $<10^7\ M_\odot$, assuming a standard CO–H_2 relationship (Jáchym et al. 2013). The gas consumption timescale due to star formation (also known as the inverse of the "star formation efficiency"), computed using SFR of $1.9 \times 10^{-3}\ M_\odot$ yr^{-1} from Hα, and the sum of H I+H_2 masses, is 2×10^{10} yr. This timescale is similar to that in the stripped extraplanar gas of three Virgo spirals (Vollmer et al. 2012), and several times longer than the

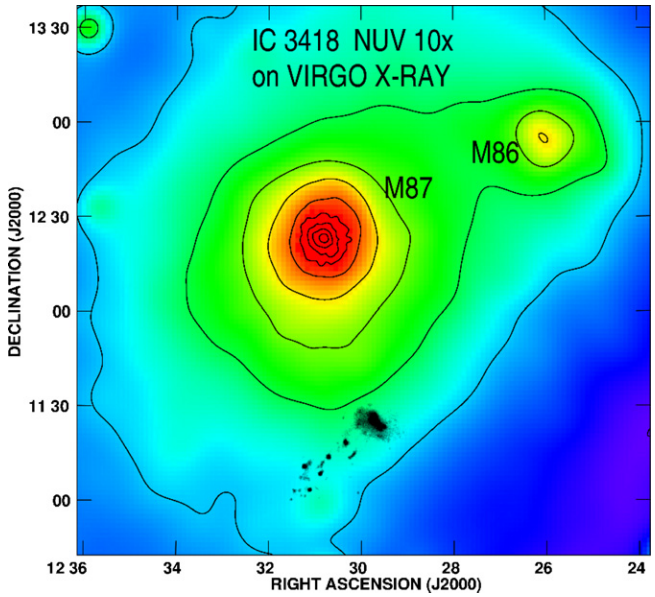

Figure 15. *GALEX* NUV grayscale image of IC3418, increased in scale by factor of 10, on *ROSAT* X-ray contour map of Virgo Cluster. Contour increment is factor of two. The position of the nucleus of the main body of IC3418 is correct.

(A color version of this figure is available in the online journal.)

timescale in typical spiral disks. This long timescale (or low "efficiency") indicates that most of the stripped gas does not form stars but remains gaseous and ultimately joins the ICM.

X-ray and diffuse Hα emission are undetected in the tail (Jáchym et al. 2013). The upper limits on mass depend on the filling factors assumed, but for reasonable choices, the upper limits are $4 \times 10^7\ M_\odot$ for X-ray emitting hot gas and $6 \times 10^7\ M_\odot$ for Hα-emitting warm diffuse gas (Jáchym et al. 2013). The lack of X-ray emission might be partly due to a low thermal pressure in Virgo, compared to other clusters where X-ray tails have been observed, resulting in a lower X-ray emissivity for the gas (Tonnesen et al. 2011). On the other hand, the tail does seem to have a low gas content. It could be in an advanced evolutionary state, as there is no longer any gas from the galaxy to supply the tail. There may be gas located downstream from the observed young stars in the tail, a real possibility given the low velocities of H II regions in the tail.

4.4. Orbit within the Cluster

The small projected radial distance of IC3418 from M87 and the presence of a gas-stripped tail support the idea that IC3418 may be near its closest approach to M87. IC3418 is moving toward us with respect to the cluster center at 900 km s^{-1}. This moderately high line-of-sight velocity implies that the galaxy is located somewhere between the cluster center and intermediate clustercentric distances but not near apocenter, where a near-zero line-of-sight velocity would be expected.

Figure 15 shows a NUV image of IC3418 on a map of the Virgo Cluster. If ICM motions are small, the tail indicates the projected direction of motion of IC3418 through the cluster. Figure 15 shows that the tail position angle of 132° is offset by 115° from the vector connecting IC3418 and M87. The component of orbital motion in the plane of the sky is thus ~two times more tangential than radial. This is different from several Virgo spiral galaxies at larger projected distances (500–800 kpc), which have gas tails pointing roughly radially away from M87 (Chung et al. 2007). These are thought to be galaxies on highly radial orbits which are falling into the cluster for the first time. Since their projected tails have large radial components, they are likely far from closest approach. In contrast, the projected tail angle in IC3418 is more tangential than radial. If this is also true for the 3D tail angle, then IC3418 would be near closest approach, although projection effects can be misleading.

We have calculated cluster orbits consistent with the observed orbital components of IC3418: the line-of-sight velocity, and the plane of sky position and direction of motion, the latter inferred from the tail angle. The free parameters of the models are the current line-of-sight position of IC3418 and the amplitude of its plane of sky velocity. We assume a smooth and spherically symmetric mass distribution for the Virgo Cluster, represented with a radial β profile (Schindler et al. 1999). The cluster mass distribution is truncated at 2 Mpc distance. Based on the likelihood of IC3418's location near pericenter, as explained above, we have varied the current line-of-sight position relative to M87 in the interval of $(-500, 500)$ kpc. The sky plane velocity varied from 700 to 1400 km s^{-1}, resulting in radial orbits with peri-to-apocenter ratios changing from about 1:5 to 1:20. Velocities outside this range would yield either too compact or too prolonged (close-to unbound) orbits. Fast orbits at large distances from M87, or slow orbits close to M87 are also less probable from the point of view of distribution of orbits in galaxy clusters (Benson 2005). All consistent orbits have IC3418 within about 350 Myr of closest approach to M87. While the observed orbital components and the simulated orbits cannot determine whether it is currently before or after pericenter passage, it is statistically more likely to have a line-of-sight position relative to M87 of $\leqslant$300 kpc than a distance as large as 500 kpc.

Additional orbital constraints come from the observation of recent quenching in IC3418. Since most of the gas removal from the disk occurs before pericenter passage, the quenching time of 300 ± 100 Myr in the center of IC3418 suggests that the galaxy is presently no more than 400 Myr after pericenter, and possibly still before pericenter. The presence of H I at the observed position in the tail, only 14 kpc from the main body, suggests that IC3418 is in a pre-pericenter stage. The modeling of (Jáchym et al. 2013) suggests that parcels of gas with column densities typical for H I would be stripped to much larger distances after pericenter. The presence of fireballs, which are unusual in the Virgo Cluster, suggests an extreme ram pressure for Virgo, and this also argues for a current position close to the core.

An upper limit on the current ram pressure felt by IC3418 is ~1800 cm^{-3}(km s^{-1})^2, assuming a smooth static ICM, a sky plane velocity of 1400 km s^{-1}, and a distance from M87 equal to its projected distance. If the adopted position angle P.A. = 50° and inclination $i = 30°$ of IC3418 are correct, the wind angle is currently within 25° of face-on, for all consistent orbits, if the SE side of the disk is the near side. The 3D length of the tail is 1.2–1.7 times larger than its projected length, if the plane of sky velocity is between the reasonable limits of 700–1400 km s^{-1}, as suggested above.

Ram pressure of this strength is sufficient to strip gas with a surface density of $15\ M_\odot$ pc^{-2} from the center of IC3418 or $50\ M_\odot$ pc^{-2} at a distance of 5 kpc from the center but is insufficient to strip giant molecular clouds (GMCs) with surface densities of $\sim 100\ M_\odot$ pc^{-2} (Jáchym et al. 2013). Thus, dense clouds in the disk of IC3418 likely decoupled from surrounding lower density gas which was stripped, and then were either ablated by Kelvin–Helmholtz instabilities, or evolved to a lower density state that was directly stripped (Crowl et al. 2005;

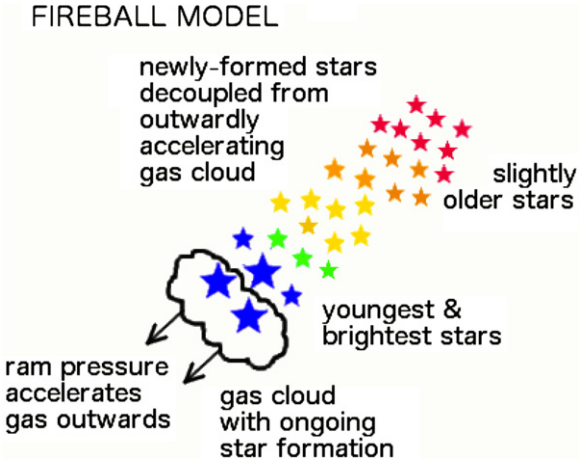

Figure 16. A cartoon of our fireball model. A gas cloud is accelerated outward by ongoing strong ram pressure. It is trailed by young stars that formed in the gas cloud but are now decoupled from the gas since the stars do not feel the ram pressure. The stellar associations nearest the gas cloud are the youngest, so still contain the most massive and luminous stars, and this forms the luminous head of the head–tail source (or "knot"). Further from the gas cloud are slightly older stellar associations which no longer contain the most massive and luminous stars, and this forms the tail (or "filament"). The color differences of the stars along the tail are greatly exaggerated.

(A color version of this figure is available in the online journal.)

Abramson & Kenney 2013). The dense star-forming clouds in the tail would not have originated from disk GMCs which were directly stripped but instead formed locally in the tail via cooling (Tonnesen & Bryan 2012). Because of the much lower gravitational forces in the tail, GMCs which form in the tail can be directly accelerated by ram pressure, and this likely plays an important role in the fireball phenomenon.

5. DISCUSSION

5.1. Fireballs and Linear Stellar Streams

The positions of the H II regions at the outer heads of UV-bright head–tail and linear stellar streams ("fireballs") strongly suggest a scenario in which star-forming gas clouds continue to be accelerated outward by ram pressure, depositing newly formed stars behind it on its path. The stars are unaffected by the ram pressure, so the stars separate from the gas cloud. Once stars decouple from gas, they may fall back into the galaxy following ballistic orbits (Hester et al. 2010) if their birth cloud had not achieved escape velocity. Such fallback stars would add to the galaxy's halo or thick disk (Abramson et al. 2011) but not principally to its bulge, as was suggested by Kapferer et al. (2009).

We show a cartoon of our fireball model in Figure 16. It shows an outwardly accelerating gas cloud, trailed by decoupled young stars. The stellar associations nearest the gas cloud are the youngest, so they still contain the most massive and luminous stars. This forms the luminous head of the head–tail source (or "knot"). Further from the gas cloud are slightly older stellar associations which no longer contain the most massive and luminous stars, and this forms the tail (or "filament"). Followup studies are needed to confirm this predicted stellar age gradient in the head–tail sources. We note that within a galaxy, the large gravitational restoring force can prevent dense star-forming GMCs from being directly stripped by ram pressure. But far from the galaxy in the tail, the gravitational restoring force is weak, and this makes it easier to accelerate star-forming GMCs by ram pressure.

Stars that form in the tail will have the same initial velocity as the parental gas cloud, and both are subject to the same gravitational acceleration from the galaxy. The only difference is that the gas clouds continue to be accelerated by ram pressure, but the stars are not. Thus, the timescale $t_{\rm stream}$ for creating a linear stellar stream of length L by ram pressure acceleration $a_{\rm ram}$ of a (decoupled) gas cloud of surface density $\Sigma_{\rm gas}$ is $t_{\rm stream} = (2L/a_{\rm ram})^{1/2}$ (Hester et al. 2010), or

$$t_{\rm stream} = \sqrt{\frac{2L\,\Sigma_{\rm gas}}{\rho_{\rm ICM}\,v^2}}. \quad (2)$$

For a GMC-like gas surface density of $\Sigma_{\rm gas} = 100\,M_\odot$ pc^{-2}, an ICM density $\rho_{\rm ICM}$ of 10^{-3} cm^{-3}, and a relative velocity v of 1400 km s^{-1}, it takes $t_{\rm stream} = 60$ Myr to create a stellar stream with $L = 1$ kpc. With such an age difference between the head and the tail, a gradient in optical/UV colors should be detectable with sufficient sensitivity. For the linear stream UV3, which has a length of ~2 kpc, Hester et al. (2010) measure a UV color gradient corresponding to an age gradient of ~100 Myr. This is in good agreement with our estimate. Stellar streams are expected to be longer in clusters with higher ram pressure. This seems to be the case for the Coma galaxy RB 199, which has some streams as long as 10–20 kpc, (Yoshida et al. 2008), much longer than those in IC3418, presumably because the ram pressures in Coma are much higher than in Virgo (Hester et al. 2010). Streams are generally longer in the inner tail of IC3418 than the outer tail. Two effects may contribute to this difference: the outer tail streams are still forming, and the inner tail streams are tidally stretched, since close to the disk the gradient of restoring force along the filament is larger than at larger z distances.

An alternative way to make linear stellar streams is to make linear streams of dense gas by ram pressure. This could happen via differential acceleration of gas elements with different densities, forming a linear gas stream which then cools and forms stars along its length. This process may happen in some galaxies. RB199 exhibits both head–tail features like those in IC3418, with relatively compact Hα concentrations at the head of a linear stream of young stars pointing back toward the galaxy, but also some linear Hα features as long as 18 kpc. The linear Hα features in RB199 are preferentially in the outer part of the tail and are fainter in the UV–optical than the inner tail features, suggesting that they are lower mass features which form a small fraction of the tail stars. We attribute the differences between RB199 and IC3418 to stronger ram pressures in the Coma cluster.

5.2. How IC3418 Compares to other Galaxies with Ram Pressure Stripped Tails

Several Virgo spiral galaxies have tails of H I gas produced by ram pressure stripping (Kenney et al. 2004; Oosterloo & van Gorkom 2005; Crowl et al. 2005; Chung et al. 2007; Abramson et al. 2011), and some of these have UV and Hα sources from recent star formation in the tails (Kenney & Koopmann 1999; Cortese et al. 2004; Crowl et al. 2005; Abramson et al. 2011). But unlike IC3418 none of these Virgo spirals are completely gas-stripped, none have such a luminous UV tail, and none have fireballs or linear stellar streams produced by ram pressure. The Virgo spiral NGC 4330 is similar to IC3418 in having an extraplanar UV tail, and H II regions only in the outer part of the UV tail (Abramson et al. 2011). But IC3418 differs

from NGC 4330 in having a symmetric UV tail, as well as fireballs in the tail. IC3418 is ∼1–2 mag fainter and has 10 times less stellar mass than the prototypical stripping-in-action Virgo spirals NGC 4522, NGC 4402, and NGC 4330 (Kenney et al. 2004; Crowl et al. 2005; Abramson et al. 2011). The spirals in Virgo may be too massive to be so completely and dramatically stripped. The dwarf IC3418 is both lower in mass and closer to the cluster center (at least in projection)[11] than the other Virgo galaxies known to be experiencing ram pressure stripping.

The phenomenon of one-sided tails of young stellar knots and parallel linear stellar streams has been seen in more distant clusters. Numerous galaxies with one-sided tails of Hα emission or young stellar knots and parallel linear stellar streams have been observed in the Coma cluster (Yoshida et al. 2008; Yagi et al. 2010; Smith et al. 2010b; Fossati et al. 2012). Cortese et al. (2007) have described two peculiar galaxies falling into the massive $z \sim 0.2$ galaxy clusters Abell 1689 and Abell 2667, each with extraordinary one-sided tails of bright blue knots and stellar streams. Two spiral galaxies in the Norma cluster (ESO137) have very prominent X-ray and Hα ram pressure stripped tails (Sun et al. 2010). We think all these galaxies are observed in a short-lived phase of very strong ram pressure stripping in which a large fraction of the ISM is stripped out. These galaxies are all more massive than IC3418, but their clusters are also more massive, with denser ICMs than Virgo, and have peak ram and ICM thermal pressures ∼10–100 times that in Virgo. It may be that rapid strong stripping can occur for large galaxies in massive clusters, but only for dwarf galaxies in less massive clusters like Virgo.

Features which resemble linear stellar streams are seen in the simulations of both Kapferer et al. (2009) and Tonnesen & Bryan (2012), and head–tail features, with young stars at the heads of elongated stellar streams, are clearly seen in the Kapferer et al. (2009) simulations (although not commented on in their paper). Both the ram pressure and thermal pressure seem to be important for producing the star formation in the tails and the linear stellar streams. Kapferer et al. (2009) and Tonnesen & Bryan (2012) both find that the amount of star formation in the tail is higher when the ambient thermal ICM pressure is higher, presumably since gas clouds experiencing external pressure can collapse more readily. Both increase toward the center of the cluster, and this could be why IC3418 but not the Virgo spirals show pronounced stellar streams at larger projected distances. The lower gravitational potential of IC3418 may also be relevant, since with the same ram pressure its gas can be more easily accelerated and stripped.

5.3. Other Ram Pressure Stripped Virgo Dwarfs

There are other Virgo dwarf galaxies which have been proposed to be ram pressure stripped. The dwarf UGC7636=VCC1249, located very close to the large Virgo elliptical M49, is likely experiencing the combined effects of tidal and ram pressure stripping due to a collision with M49 (McNamara et al. 1994; Lee et al. 2000; Arrigoni Battaia et al. 2012). Optical images show that the outer parts of the dwarf's stellar body are distorted in a way consistent with a tidal interaction, while the morphology of the inner region is bow shaped at the apparent leading edge, suggestive of ram pressure. There is no H I in the stellar body, but there is an H I cloud nearby, between M49 and the dwarf in both space and velocity. The dwarf's gas has likely been stripped by ram pressure from the gaseous halo of M49. While an excellent case for ram pressure stripping, UGC7636 is stripped by the halo of M49 rather than the general Virgo ICM, and since it passes close to M49, it has experienced a strong tidal interaction that accompanies the ram pressure stripping. Most cluster dwarfs are likely stripped by the general ICM rather than the ISM of galaxies.

There are a few Virgo dIs, detected but deficient in H I, that seem partially stripped and are candidates for active stripping by the cluster ICM. The Virgo dI IC3365, located 3.5° from M87, shows evidence for ongoing ram pressure stripping. Its H I content is ∼5–10 times lower than most dIs, with $M_{\rm HI}/L_{\rm B} = 0.3$, and its H I contours seem compressed on one side (Skillman et al. 1987). Lee et al. (2003) identified five Virgo dIs with lower gas mass fractions at a given oxygen abundance than non-cluster dI's. These galaxies are H I-deficient by factors of 7–30 and are among the dIs located closest to the cluster center. While these are good candidates for active stripping, none are known to have tails of only gas and young stars, which is a clear signature of active ram pressure stripping.

There are numerous early type dwarfs which are candidates for post-stripped galaxies. In an early study, Vigroux et al. (1986) proposed that the large dwarf IC3475 with an uncertain classification (ImIV or dE1 pec according to Binggeli et al. 1985) is ram pressure stripped. It has no H I or ongoing star formation (Hα) detected to low limits, although it has substructure in the disk (a bar and knots) and intermediate optical colors which are bluer than most dEs ($B - R = 1.5$) but are sufficiently red that star formation must have stopped $\geqslant$1 Gyr ago. It is located very close (in projection) to the cluster center, only 35′ from M87, although if the quenching time is $\geqslant$1 Gyr, then it must have been stripped before current core crossing. It remains an excellent candidate for a previously stripped dwarf and may be similar to dEs with low-level disk substructure. Jerjen et al. (2000) discovered spiral structure in the dE IC3328, which could be a gas-stripped dI. Nearly 10% of 476 Virgo dEs in an Sloan Digital Sky Survey (SDSS) imaging study show low-level disk substructure including spiral arms, bars, and edge-on disks (Lisker et al. 2006b), and roughly 5% show blue centers indicating recent star formation (Lisker et al. 2006a) with much higher fractions for the brightest dEs. Both populations are consistent with being gas-stripped dIs.

While these galaxies are good examples of likely ram pressure stripping of dwarfs in Virgo, IC3418 is an even better example because it has clear-cut evidence for active ram pressure, it is (almost) completely stripped, and it is stripped by the Virgo ICM.

5.4. DIs→dE's by Ram Pressure Stripping

We propose that IC3418 is a dI which was very recently almost completely stripped of its gas by ram pressure. As its last generation of stars fades and reddens and as the substructure within the stellar disk disperses, the galaxy will presumably become a dE.

Many previous studies have concluded that ram pressure stripping of infalling dIs is a likely origin or partial origin for cluster dEs (Lee et al. 2003; van Zee et al. 2004a, 2004b; Boselli et al. 2008; Kormendy & Bender 2012). dEs and dIs have similar masses and follow similar scaling relationships for their luminosity and radial stellar light distributions, including the

[11] Located 1.°0 from the cluster center, IC3418 is closer to the cluster center, in projection, than all the Virgo spirals known with ram pressure stripped tails, which are located at 1.°3–3.°5 from the cluster center. It has the same projected distance as the gravitationally disturbed spiral NGC 4438, which may be experiencing ram pressure stripping from the cluster (Vollmer et al. 2009) but has also experienced a damaging high-velocity collision with M86 (Kenney et al. 2008), so its case is complicated.

shape of the radial profiles (close to exponential), central surface brightnesses, and scale lengths (Lin & Faber 1983; Lee et al. 2003; Kormendy & Bender 2012). The parameter correlations of absolute magnitude, effective radius, and surface brightness are very similar for dIs and dEs, and quite distinct from ellipticals (Kormendy & Bender 2012). Dwarf galaxies ($10^7 < M < 10^9\ M_\odot$) with no active star formation are extremely rare in the field, and the fraction of quenched dwarf galaxies decreases rapidly with increasing distance from a massive host (Geha et al. 2012). This indicates that some interaction in a dense environment, rather than any internal mechanism, is responsible for quenching star formation in dwarfs.

IC3418 follows the scaling relation for other dIs and dEs. Given its exponential light profile with scale length of $19'' = 1.5$ kpc, and its central surface brightness of 23 B mag arcsec^{-2}, and its B magnitude of -16.5, it falls in with other dwarfs in Figure 19 of Lee et al. (2003).

Thus, the faded remnants of IC3418 and other gas-poor dI's in Virgo should closely resemble at least some of the dEs currently seen in the cluster core (Lee et al. 2003), particularly the dEs with blue centers (Lisker et al. 2006a) or disk substructure (Lisker et al. 2006b). Blue centers are naturally produced by non-instantaneous ram pressure stripping since galaxies are stripped from the outside in. While some of the blue center dEs could also have had tidally triggered central star formation, their lack of gas is likely due to ram pressure stripping. IC3418 has a color gradient of 0.15 in $g-r$ (Hester et al. 2010), which exceeds that which is required to be defined a blue centered dE by Lisker et al. (2006a), so it could evolve to become one of blue center dEs. Since it has spiral structure and a disk, it could also evolve to become one of the disk substructure dEs of Lisker et al. (2006b).

Objections to the ram pressure stripping scenario for the origin of cluster dEs are based on differences between the dI and dE populations that cannot be accounted for by ram pressure alone, including kinematics, shapes, metallicity, and nuclei (Ferguson & Binggeli 1994; Conselice et al. 2001). These real differences indicate that tidal interactions and perhaps other mechanisms have also played an important role in the evolution of most dEs (Kormendy & Bender 2012).

For example, ram pressure stripping cannot explain the observed differences in stellar kinematics between these galaxy classes. dIs are rotationally supported, with $v/\sigma \geqslant 1$, whereas dEs have heterogenous kinematics. Some have rotation and some do not. All known dEs have $v/\sigma \leqslant 1$ (Geha et al. 2003; van Zee et al. 2004b). These kinematic differences seemingly require gravitational interactions for at least some of the dEs. Numerical simulation have suggest that "galaxy harassment" (Moore et al. 1998; Mastropietro et al. 2005), the accumulation of gravitational heating via multiple minor encounters, can transform a rotationally supported galaxy into a dispersion supported galaxy (although the importance of this effect has been questioned by Smith et al. 2010a). Careful photometric analysis by Kormendy & Bender (2012) shows that some Virgo dEs have clearly puffed-up outer disks consistent with tidal interactions.

Many dEs have nuclei (Côté et al. 2006), which are rare in dIs of the same mass (Binggeli et al. 1987; Ferguson & Binggeli 1994) although they are common in more massive Sd and Sm galaxies (Böker et al. 2004; Kormendy & Bender 2012). Whereas dIs and non-nucleated dEs have the same shape distributions, nucleated dEs may be rounder on average (Ferguson & Sandage 1989; Lisker et al. 2007). These facts suggest that the progenitors of nucleated dEs are more massive Sd and Sm galaxies and that the dE has lost mass and become rounder over time due to tidal interactions (Kormendy & Bender 2012).

Until recently, it was thought that dSphs and dEs had somewhat higher metallicities than dIs of the same luminosity or mass, suggesting that dSphs had undergone comparatively more early and rapid star formation episodes (Mateo 1998; Grebel et al. 2003; Freeland & Wilcots 2011). However this was based on photometric estimates of metallicities, which can suffer from systematic errors. A newer study based on spectroscopic metallicities shows that dIs and dSphs in the Local Group obey the same mass–metallicity relation (Kirby et al. 2013). Similar mass–metallicity relations for dIs and dEs agrees with the results of Weisz et al. (2011), who find similar star formation histories for nearby early and late types dwarfs. They find that the average dwarf formed ∼50% of its stars by $z \simeq 2$ and ∼60% by $z \simeq 1$, regardless of morphological type. The mean star formation histories of dIs, transition galaxies, and dSphs are similar over most of cosmic time and only began to diverge a few Gyr ago with the clearest differences appearing during the most recent 1 Gyr (Weisz et al. 2011). We note that identical mass-luminosity relations for all dIs and dEs might not be expected, if some dEs have lost mass through tidal interactions, as seems likely.

dEs are a heterogenous population with a range of evolutionary histories (Lisker et al. 2007), and tidal interactions have clearly helped shape a large fraction of dEs. But the one thing they have in common is a lack of gas and star formation, and this is probably caused in most cases by ram pressure stripping, since tidal interactions do not selectively remove gas.

It is clear that ram pressure stripping is not the only interaction which has affected most of the cluster dEs. Simulations of local group dwarfs indicate that both ram pressure stripping and tidal interactions need to occur to account for all properties (Mayer et al. 2007). In the dense cluster environment, it is only natural and even expected that most galaxies should experience both ram pressure stripping and tidal interactions, *although generally at different times.*For most cluster dwarfs, removal of all or most of the gas probably occurs during one ram pressure stripping event during its first approach to the core. Gas removal is generally a single event localized in time and space and is decisive for the dI→dE transformation. In contrast, tidal interactions can occur as pre-processing before the first infall, during the first infall, and on any subsequent orbit. Tidal damage and mass loss can increase through multiple interactions and be widely spread over time and cluster locations and orbits. Significant tidal damage can occur after the first infall, when gas is stripped. Although tidal interactions are important for dwarf galaxy evolution and responsible for some dE properties, they are not decisive for the dI→dE transformation.

dIs are those dwarf galaxies that have been in cluster the least amount of time and have never been through the cluster center. These galaxies are expected to be much less tidally disturbed than dEs, on average. Once a gas-rich dwarf enters the central part of a cluster like Virgo, it will be largely gas-stripped. The widespread ram pressure stripping of spirals in Virgo, in which massive spirals that get within ∼0.5 Mpc of the cluster core, typically get stripped to 0.3–0.7R_{25} (Koopmann & Kenney 2004; Chung et al. 2009), implies that dwarfs, with their shallower gravitational potentials, should be completely or nearly completely stripped on its first core passage.

dEs are those dwarf galaxies that have been in cluster for longer than the dIs, and the subpopulation of dEs which are nucleated, centrally concentrated, and slow-moving may be the oldest subpopulation (Lisker et al. 2009). dEs in general have been fully (or nearly fully) stripped of their gas[12] and have made one or more orbits in the cluster, subjecting themselves to multiple tidal encounters with the cluster and other galaxies. Such encounters tidally strip the outer galaxy, and dynamically heat the bound stars. The gravitational disturbance histories of cluster dwarfs vary, dominated by a few discrete events, and each event can be different, depending on the separation and relative velocity at closest approach and on the angles and angular momenta of the interaction. This may help explain why dEs are not a homogenous class (Lisker et al. 2006b, 2006a, 2007, 2008). While there may be different pathways to make the different kinds of dEs, gas stripping is likely necessary for all.

While the lack of gas and star formation and associated substructure is not the only difference between dIs and dEs, it is the single most important difference since it determines whether a galaxy is a dI or dE. A galaxy which experiences gas stripping but not a tidal interaction would (ultimately) be classified as a dE or dSph, whereas a galaxy which experiences a tidal interaction but not gas stripping would not be classified as dE or dSph.

We propose that IC3418 is caught red-handed in that critical part of the dI→dE transformation—the removal of its gas by ram pressure stripping.

6. SUMMARY

1. IC3418's tail is one-sided, straight, and centered on the main body of galaxy, unlike tidal tails. There is no evidence of a smoother, older stellar component to the tail, as would exist in a tidal tail. All detected stars are clustered and young, which is consistent with all the tail stars originating from star formation within a ram-pressure stripped gas tail. A deep optical image indicates no strong gravitational disturbance to the main stellar body, which is further evidence that the tail is the product of ram pressure stripping of gas.
2. Many UV tail features are linear, parallel streams of young stars. Some of them are head–tail features, with a knot of UV-bright stars at the outermost head of a linear stellar stream. Hα emission is located at the heads of these, outwardly offset by ~80–150 pc from the UV peaks. The head–tail ("fireballs") and linear stellar features in the stripped tail are likely formed from dense gas clumps which continue to accelerate through ram pressure, leaving behind streams of newly formed stars which are not affected by ram pressure.
3. H II regions in the tail have line-of-sight velocities 40–115 km s^{-1} higher than the galaxy. This velocity offset is in the direction expected for ram pressure stripping, as IC3418 is moving toward us through the cluster at 900 km s^{-1}. The velocities are relatively low and much closer to the galaxy than the cluster ICM. This implies that gas in the tail is still experiencing strong ram pressure, which is likely necessary to form the head–tail features ("fireballs"). In simulations ram pressure stripped tails extend closer to the ICM velocity, suggesting that the tail in IC3418 is much longer than the currently known tail and that star formation happens only in the inner part of the tail.
4. Most of the outer tail features have velocities which exceed the escape velocity and will join intracluster space. Some of the inner tail features likely remain bound to the galaxy and should ultimately fall back in. Some of the infalling stars will be in the form of extended halo streams, which differ in character from tidal halo streams in being clumpy, young, and with possible age gradients. One likely infalling halo stream is identified in the UV image. Compared to the other tail streams, it is closer to the galaxy but further from the tail centroid, slightly curved, redder in color, and of lower surface brightness.
5. We identify three distinct zones in the tail. The inner tail has UV-bright linear streams and knots but no head–tail features and very little Hα emission. The outer tail has UV-bright head–tail features, i.e., knots with Hα at the heads of linear stellar streams ("fireballs"). The very outer tail has lower surface brightness diffuse UV features with associated Hα emission and the highest Hα/NUV ratio. We propose the following interpretation for the different tail zones. Nearly all the gas has been stripped from the inner tail, and some stellar features here may be falling back into galaxy. The outer tail still has gas and ongoing star formation with some gas large gas concentrations being outwardly accelerated and forming fireballs. The very outer tail still has gas and ongoing star formation but has smaller gas concentrations and, therefore, less bright stellar knots.
6. While no H I has been detected from the main body of the galaxy, a small amount of H I, $4 \times 10^7\ M_\odot$, is detected from the outer tail. This corresponds to only 6% of the expected H I mass of a late type dwarf with the mass of IC3418. The gas consumption timescale due to star formation, computed from the ratio of H I mass to the Hα-based SFR, is longer than the typical values in galaxy disks, indicating that most of stripped gas does not form stars but ultimately joins the ICM. The mass of stars in the tail is only ~1% of the stellar mass of the galaxy.
7. Spectroscopy shows that some sources in the tail region are background galaxies. Light from these contaminating sources were probably included in the Fumagalli et al. (2011) SED analysis, which concluded that the ages of stellar features in the tail ranged from 80 to 1400 Myr. We confirm that some of the features with the oldest derived ages have bright contaminating background galaxies, so that some of the ages derived by Fumagalli et al. (2011) are likely overestimates. The true age range is probably closer to that of the features with the youngest derived ages being between 80 and 390 Myr. Such an age range is consistent with the star formation quenching time in the main body of the galaxy.
8. We have analyzed the stellar population of the main body of IC3418 as a function of radius through optical spectroscopy and UV photometry. Assuming a star formation history with a constant SFR until the time of quenching, with a possible burst at quenching time, we find the quenching time in the galaxy center was 300 ± 100 Myr ago. A starburst occurred near the time of quenching, with a global average of

[12] While most dEs are gas-poor and undetected in H I, a small fraction of dEs in Virgo (4%–15%) are detected in H I (Conselice et al. 2003; Hallenbeck et al. 2012), with values of $M_{\rm H\,I}/M_{\rm stars}$ similar to those of late type galaxies. Nearly all have projected locations in the cluster outskirts. Of the 12 dEs detected in H I by the ALFALFA survey, 6 are blue and are likely misclassified dIs and 6 are red and may be best explained by quiescent galaxies (possibly previously stripped) which have recently accreted H I (Hallenbeck et al. 2012).

10% ± 5% of the stars formed in the burst, although this varies with the position in the galaxy. Older quenching times at larger radii are expected from ram pressure stripping, as galaxies are stripped from the outside in. The FUV/NUV ratio in IC3418 suggests a modest radial gradient in quenching time of 70 Myr from 0″–48″, indicating that it was stripped rapidly. Stars in the galaxy have a subsolar metallicity of $0.6 \pm 0.2\ Z_{\odot}$. Spectroscopy of H II regions in the tail suggest gas metallicities of 0.36–0.53 $Z_{\odot}$, which is similar to the stars in the main body.

9. We propose that IC3418 is a dI that was very recently almost completely stripped of its gas by ram pressure. Neither Hα nor H I emissions are detected in the main body of the galaxy, despite the presence of spiral arms and features resembling star-forming regions. As its last generation of stars fades and reddens and as the substructure within the stellar disk disperses, the galaxy will presumably become a dE. Since IC3418 has a color gradient, it could evolve to become one of blue center dEs discussed by Lisker et al. (2006a), and since it has spiral structure and a disk, it could become one of the disk substructure dEs of Lisker et al. (2006b).
10. An unresolved source near the galaxy center with $M_V = -9.4$ and $B - V = 0.08$ has a velocity which matches the galaxy, and may be a nuclear star cluster. Photometry of other unresolved bright sources in the direction of IC3418 reveal that several of them are too bright to be supergiants in IC3418, so are likely foreground Milky Way stars. Others could be either foreground stars, or supergiants or globular clusters in IC3418.
11. We propose that the "fireball phenomenon" seen in IC3418 is not the default mode of ram pressure stripping in the Virgo Cluster but probably arises from very strong ram pressure, which is what IC3418 is likely experiencing since it is probably close to the cluster core. Many spiral galaxies in Virgo are known to be experiencing ram pressure but do not have UV-bright tails or fireballs. The other galaxies with known UV-bright tails and fireballs are in more massive clusters with stronger ram (and thermal) pressure.
12. We point out that both ram pressure stripping and tidal interactions are required to explain the properties of most dEs. Ram pressure stripping is decisive for forming a dE since ram pressure stripping without tidal interactions will make a dE, but a tidal interaction without ram pressure stripping will not make a dE. Some dEs have properties consistent with only ram pressure stripping but no significant tidal interaction. Dwarf galaxies in clusters are expected to experience both ram pressure stripping and tidal interactions, but the timing of the interactions will generally be different. Ram pressure stripping occurs once upon first cluster infall, and tidal interactions are expected to occur multiple times, both before and after first infall, with tidal damage increasing over time.

We are grateful to the staffs of the WIYN and Keck observatories for their assistance obtaining the data. This research has made use of the GOLD Mine Database (Gavazzi et al. 2003), and of the NASA/IPAC Extragalactic Database (NED) which is operated by the Jet Propulsion Laboratory, California Institute of Technology, under contract with the National Aeronautics and Space Administration. P.J. acknowledges support from Project M100031203 of the Academy of Sciences of the Czech Republic. We thank the anonymous referee for comments that helped improve the manuscript.

Facilities: Keck:I, Keck:II, WIYN, GALEX

REFERENCES

Abramson, A., & Kenney, J. D. P. 2013, AJ, in press
Abramson, A., Kenney, J. D. P., Crowl, H. H., et al. 2011, AJ, 141, 164
Arrigoni Battaia, F., Gavazzi, G., Fumagalli, M., et al. 2012, A&A, 543, 112
Benson, A. J. 2005, MNRAS, 358, 551
Binggeli, B., Sandage, A., & Tammann, G. A. 1985, AJ, 90, 1681
Binggeli, B., Tammann, G. A., & Sandage, A. 1987, AJ, 94, 251
Böker, T., Sarzi, M., McLaughlin, D. E., et al. 2004, AJ, 127, 105
Boselli, A., Boissier, S., Cortese, L., & Gavazzi, G. 2008, ApJ, 674, 742
Chung, A., van Gorkom, J., Kenney, J., Crowl, H. H., & Vollmer, B. 2009, AJ, 138, 1741
Chung, A., van Gorkom, J., Kenney, J., & Vollmer, B. 2007, ApJL, 659, L115
Conselice, C. J., Gallagher, J. S., III, & Wyse, R. F. G. 2001, AJ, 122, 2281
Conselice, C. J., O'Neil, K., Gallagher, J. S., III, & Wyse, R. F. G. 2003, ApJ, 591, 167
Cortese, L., Gavazzi, G., Boselli, A., & Iglesias-Paramo, J. 2004, A&A, 416, 119
Cortese, L., Marcillac, D., Richard, J., et al. 2007, MNRAS, 376, 157
Côté, P., Piatek, S., Ferrarese, L., et al. 2006, ApJS, 165, 57
Crowl, H. H., & Kenney, J. D. P. 2006, ApJL, 649, L75
Crowl, H. H., & Kenney, J. D. P. 2008, AJ, 136, 1623
Crowl, H. H., Kenney, J. D. P., van Gorkom, J. H., & Vollmer, B. 2005, AJ, 130, 65
De Rijcke, S., Van Hese, E., & Buyle, P. 2010, ApJL, 724, L171
de Vaucouleurs, G., de Vaucouleurs, A., Corwin, H. G., Jr., et al. 1991, Third Reference Catalogue of Bright Galaxies (vol. I–III; New York: Springer)
Faber, S. M., Phillips, A. C., Kibrick, R. I., et al. 2003, Proc. SPIE, 4841, 1657
Ferguson, H. C., & Binggeli, B. 1994, A&ARv, 6, 67
Ferguson, H. C., & Sandage, A. 1989, ApJL, 346, L53
Fossati, M., Gavazzi, G., Boselli, A., & Fumagalli, M. 2012, A&A, 544, 128
Freeland, E., & Wilcots, E. 2011, ApJ, 738, 145
Fumagalli, M., Gavazzi, G., Scaramella, R., & Franzetti, P. 2011, A&A, 528, 46
Gavazzi, G., Boselli, A., Donati, A., Franzetti, P., & Scodeggio, M. 2003, A&A, 400, 451
Gavazzi, G., Boselli, A., Cortese, L., et al. 2006, A&A, 446, 839
Gavazzi, G., Boselli, A., van Driel, W., & O'Neil, K. 2005, A&A, 429, 439
Geha, M., Blanton, M. R., Yan, R., & Tinker, J. L. 2012, ApJ, 757, 85
Geha, M., Guhathakurta, P., & van der Marel, R. P. 2002, AJ, 124, 3073
Geha, M., Guhathakurta, P., & van der Marel, R. P. 2003, AJ, 126, 1794
Geha, M., van der Marel, R. P., Guhathakurta, P., et al. 2010, ApJ, 711, 361
Gil de Paz, A., Boissier, S., Madore, B. F., et al. 2007, ApJS, 173, 185
Grebel, E. K., Gallagher, J. S., III, & Harbeck, D. 2003, AJ, 125, 1926
Hallenbeck, G., Papastergis, E., Huang, S., et al. 2012, AJ, 144, 87
Hester, J. A., Seibert, M., Neill, J. D., et al. 2010, ApJL, 716, L14
Hoffman, G. L., Williams, H. L., Salpeter, E. E., Sandage, A., Binggeli, B., et al. 1989, ApJS, 71, 701
Jáchym, P., Kenney, J. D. P., Ržuička, A., et al. 2013, A&A, 556, 99
Jerjen, H., Kalnajs, A., & Binggeli, B. 2000, A&A, 358, 845
Kapferer, W., Sluka, C., Schindler, S., Ferrari, C., & Ziegler, B. 2009, A&A, 499, 87
Kenney, J. D. P., & Koopmann, R. A. 1999, AJ, 117, 181
Kenney, J. D. P., Tal, T., Crowl, H. H., Feldmeier, J., & Jacoby, G. H. 2008, ApJL, 687, L69
Kenney, J. D. P., van Gorkom, J. H., & Vollmer, B. 2004, AJ, 127, 3361
Kirby, E. N., Cohen, J. G., Guhathakurta, P., et al. 2013, ApJ, 779, 102
Koopmann, R., & Kenney, J. D. P. 2004, ApJ, 613, 866
Kormendy, J., & Bender, R. 2012, ApJS, 198, 2
Lee, H., McCall, M. L., & Richer, M. G. 2003, AJ, 125, 2975
Lee, H., Richer, M. G., & McCall, M. L. 2000, ApJL, 530, L17
Leitherer, C., Schaerer, D., Goldader, J. D., et al. 1999, ApJS, 123, 3
Lin, D. N. C., & Faber, S. M. 1983, ApJL, 266, L21
Lisker, T., Glatt, K., Westera, P., & Grebel, E. K. 2006a, AJ, 132, 2432
Lisker, T., Grebel, E. K., & Binggeli, B. 2006b, AJ, 132, 497
Lisker, T., Grebel, E. K., & Binggeli, B. 2008, AJ, 135, 380
Lisker, T., Grebel, E. K., Binggeli, B., & Glatt, K. 2007, ApJ, 660, 1186
Lisker, T., Janz, J., Hensler, G., et al. 2009, ApJ, 706, 124L
Martin, D. C., Fanson, J., Schiminovich, D., et al. 2005, ApJL, 619, L1
Mastropietro, C., Moore, B., Mayer, L., et al. 2005, MNRAS, 364, 607
Mateo, M. L. 1998, ARA&A, 36, 435
Mayer, L., Kazantzidis, S., Mastropietro, C., & Wadsley, J. 2007, Natur, 445, 738

McLaughlin, D. E. 1999, ApJL, 512, L9
McNamara, B. R., Sancisi, R., Henning, P. A., & Junor, W. 1994, AJ, 108, 844
Mei, S., Blakeslee, J. P., Côté, P., et al. 2007, ApJ, 655, 144
Merluzzi, P., Busarello, G., Dopita, M. A., et al. 2013, MNRAS, 429, 1747
Moore, B., Lake, G., & Katz, N. 1998, ApJ, 495, 139
Ohyama, Y., & Hota, A. 2013, ApJL, 767, L29
Oosterloo, T., & van Gorkom, J. 2005, A&A, 437, L19
Pettini, M., & Pagel, B. E. J. 2004, MNRAS, 348, L59
Roediger, E., & Brüggen, M. 2008, MNRAS, 388, 465
Schindler, S., Binggeli, B., & Böhringer, H. 1999, A&A, 343, 420
Skillman, E. D., Bothun, G. D., Murray, M. A., & Warmels, R. H. 1987, A&A, 185, 61
Smith, R., Davies, J. I., & Nelson, A. H. 2010a, MNRAS, 405, 1723
Smith, R. J., Lucey, J. R., Hammer, D., et al. 2010b, MNRAS, 408, 1417
Sun, M., Donahue, M., Roediger, E., et al. 2010, ApJ, 708, 946
Tonnesen, S., & Bryan, G. L. 2010, ApJ, 709, 1203
Tonnesen, S., & Bryan, G. L. 2012, MNRAS, 422, 1609
Tonnesen, S., Bryan, G. L., & Chen, R. 2011, ApJ, 731, 98
van Zee, L., Barton, E. J., & Skillman, E. D. 2004a, AJ, 128, 2797
van Zee, L., Skillman, E. D., & Haynes, M. P. 2004b, AJ, 128, 121
Vigroux, L., Lachieze-Rey, M., Thuan, T. X., & Vader, J. P. 1986, AJ, 91, 70
Vollmer, B., Cayatte, V., Balkowski, C., & Duschl, W. J. 2001, ApJ, 561, 708
Vollmer, B., Soida, M., Chung, A., et al. 2009, A&A, 496, 669
Vollmer, B., Wong, O. I., Braine, J., Chung, A., & Kenney, J. D. P. 2012, A&A, 543, 33
Weisz, D. R., Dalcanton, J. J., Williams, B. F., et al. 2011, ApJ, 739, 5
Yagi, M., Yoshida, M., Komiyama, Y., et al. 2010, AJ, 140, 1814
Yoshida, M., Yagi, M., Komiyama, Y., et al. 2008, ApJ, 688, 918